ORIGINAL RESEARCH

Novel Role for Pleckstrin Homology-Like Domain Family A, Member 3 in the Regulation of Pathological Cardiac Hypertrophy

Jia Liu, MD;* Xiaoxiong Liu, MD, PhD;* Xuejun Hui, BS; Lin Cai, PhD; Xuebo Li, MD; Yang Yang, MD, PhD; Shangzhi Shu, MD; Fan Wang, MD; Hao Xia, MD, PhD; Shuyan Li, MD, PhD

***Background*—**Pleckstrin homology-like domain family A, member 3 (PHLDA3), a crucial member of the PHLDA family, is involved in tumor suppression, kidney injury, liver injury, and glucose metabolism. However, the role of PHLDA3 in pathological cardiac hypertrophy and heart failure remains unclear.

***Methods and Results*—**In the present study, PHLDA3 expression was downregulated in hypertrophic murine hearts and angiotensin II-treated cardiomyocytes. Next, an in vitro study suggested, by using gain- and loss-of-function approaches, that PHLDA3 attenuates Ang II exposure-induced cardiomyocyte hypertrophy. Consistent with the cell phenotype, disruption of PHLDA3 aggravated the effects of pressure overload-induced pathological cardiac hypertrophy, fibrosis, and dysfunction. In contrast, PHLDA3 overexpression resulted in an attenuated hypertrophic phenotype. Molecular analysis revealed that PHLDA3 suppressed the activation of AKT-mTOR-GSK3β-P70S6K signaling in response to hypertrophic stress, and the blockage of AKT activation rescued these adverse pathological effects of PHLDA3 deficiency-induced by AB and Ang II, respectively, in vivo and in vitro.

***Conclusions*—**Collectively, our data indicated that PHLDA3 could ameliorate pressure overload-induced cardiac remodeling mainly by blocking the AKT signaling pathway, suggesting that PHLDA3 may represent a therapeutic target for the treatment of pathological cardiac hypertrophy and heart failure. **(*J Am Heart Assoc*. 2019;8:e011830. DOI: 10.1161/JAHA.118.011830.)**

Key Words: AKT • cardiac hypertrophy • heart failure • pleckstrin homology-like domain family A, member 3 • pressure overload • signal transduction

Heart failure is an end-stage clinical manifestation of many cardiovascular diseases, such as myocardial ischemia, hypertension, and valvular heart disease, and is a leading cause of morbidity and mortality worldwide.[1]

Pathological cardiac hypertrophy is one of the most important pathological mechanisms of heart failure, which involves the transition from compensated hypertrophy to decompensated hypertrophy induced by prolonged stimulation.[2,3] Over the past few decades, multitudinous orchestrated signaling pathways, such as the mitogen-activated protein kinase (MAPK) signaling pathway and the phosphatidylinositol 3-kinase/AKT/glycogen synthase kinase-3β signaling pathway, have been implicated in the hypertrophic process.[4–6] However, the molecular mechanisms underlying the occurrence and development of pathological cardiac hypertrophy remain to be further elucidated. Moreover, a deeper comprehension of the mechanisms and pathogenesis may identify potential intervention targets of pathological cardiac hypertrophy and heart failure.

Pleckstrin homology-like domain family A, member 3 (PHLDA3), located on mouse chromosome 1 and human chromosome 1q31,[7] encodes a 127 amino acid protein with a pleckstrin homology-only domain and belongs to the PHLDA family, which shares a common PH domain.[8] PHLDA3 is expressed ubiquitously in multiple fetal and adult tissues, including the heart.[7,9,10] As an apoptosis inducer, PHLDA3 both induces caspase-dependent apoptosis and contributes

From the Department of Cardiology, First Hospital of Jilin University, Changchun, Jilin, China (J.L., X. Li, Y.Y., S.S., F.W., S.L.); Department of Cardiology, Renmin Hospital of Wuhan University, Wuhan, China (X. Liu, H.X.); Cardiovascular Research Institute, Wuhan University, Wuhan, China (X. Liu, H.X.); Hubei Key Laboratory of Cardiology, Wuhan, China (X. Liu, H.X.); Zhongnan Hospital of Wuhan University, Wuhan, China (L.C.); Institute of Model Animal of Wuhan University, Wuhan, China (L.C.); Department of Cardiology, Second Hospital of Jilin University, Changchun, Jilin, China (X.H.); Department of Cardiology, Cang Zhou People's Hospital, Cangzhou, Hebei, China (J.L.).

Accompanying Figures S1 through S5 are available at https://www.ahajournals.org/doi/suppl/10.1161/JAHA.118.011830

*Dr Jia Liu and Dr Xiaoxiong Liu are co-first authors.

Correspondence to: Shuyan Li, MD, PhD, Department of Cardiology, First Hospital of Jilin University, No. 71 Xinmin Street, Changchun, Jilin 130021, China. E-mail: shuyanli1992@163.com

Received December 20, 2018; accepted July 12, 2019.

Clinical Perspective

What Is New?

- The expression of pleckstrin homology-like domain family A, member 3 is decreased during the development of pathological cardiac hypertrophy and heart failure.
- Pleckstrin homology-like domain family A, member 3 repressed both hypertrophic stimuli-induced cardiac remodeling in vivo and cardiomyocyte enlargement in vitro mainly by blocking the AKT signaling pathway.

What Are the Clinical Implications?

- This study broadens our understanding of the molecular mechanisms of cardiac hypertrophy and suggests a novel therapeutic target for pathological cardiac hypertrophy and heart failure.

to p53-dependent apoptosis.[8] Based on the characteristics of its tumorigenesis-related cell behaviors, PHLDA3 was reported to be associated with multiple tumors, such as lung endocrine tumors,[8] pancreatic neuroendocrine tumors,[11] primary breast cancers,[12] and prostate carcinomas.[13] Moreover, several studies have demonstrated that PHLDA3 is involved in the regulation of acute kidney injury[14,15] and liver injury[16] induced by cisplatin and tunicamycin, respectively. PHLDA3 deficiency results in islet hyperplasia, enhanced insulin secretion, and improved glucose tolerance,[11] and improving abnormal glucose metabolism can improve the prognosis of cardiovascular diseases,[17] which indicates that PHLDA3 may be involved in pathological cardiac hypertrophy and heart failure. However, the role of PHLDA3 in pathological cardiac hypertrophy and heart failure remains unknown.

In the present study, decreased PHLDA3 expression was observed in mice after aortic banding (AB) and in cardiomyocytes following Ang II stimuli. Next, the antihypertrophic effect of PHLDA3 was examined in an in vitro study. Similar results were also demonstrated in an in vivo study. Cardiomyocyte-specific knockout of PHLDA3 accelerated pressure overload-induced pathological cardiac hypertrophy, fibrosis, and dysfunction, whereas the AB-induced hypertrophic response was alleviated in cardiomyocyte-specific PHLDA3-overexpressing mice. Mechanistically, we discovered that PHLDA3 played an ameliorative role in pathological cardiac hypertrophy by inhibiting the AKT signaling pathway. Indeed, blockage of AKT activity reversed the deleterious PHLDA3 deficiency-induced phenotype of cardiac hypertrophy in vivo and in vitro. Altogether, our data suggest for the first time that PHLDA3 is a novel negative modulator of pathological cardiac hypertrophy and subsequent heart failure, mainly via its inhibition of the AKT signaling pathway.

Materials and Methods

The data, analytic methods, and study materials will be made available to other researchers for purposes of reproducing the results or replicating the procedure, on request.

Reagents

Antibodies against MEK1/2 (9122, 1:1000 dilution), p-MEK1/2$^{Ser217/221}$ (9154, 1:1000 dilution), ERK1/2 (4695, 1:1000 dilution), p-ERK1/2$^{Thr202/Tyr204}$ (4370, 1:1000 dilution), JNK1/2 (9252, 1:1000 dilution), p-JNK1/2$^{Thr183/Tyr185}$ (4668, 1:1000 dilution), P38 (9212, 1:1000 dilution), p-P38$^{Thr180/Tyr182}$ (4511, 1:1000 dilution), AKT (4691, 1:1000 dilution), p-AKT^{Ser473} (4060, 1:1000 dilution), mTOR (2983, 1:1000 dilution), p-mTOR^{Ser2448} (2971, 1:1000 dilution), GSK3β (9315, 1:1000 dilution), p-GSK3β^{Ser9} (9322, 1:1000 dilution), P70S6 kinase (2708, 1:1000 dilution), p-P70S6 kinase^{Ser371} (9208, 1:1000 dilution), PHLDA3 (4294, 1:500 dilution), and GAPDH (2118, 1:1000 dilution) were purchased from Cell Signaling Technology. The antibody against atrial natriuretic peptide (sc20158, 1:200 dilution) was purchased from Santa Cruz Biotechnology. Peroxidase-conjugated secondary antibodies (1:10 000 dilution) were purchased from Jackson ImmunoResearch Laboratories for visualization. The BCA protein assay kit was purchased from Pierce. Fetal bovine serum was purchased from Gibco (10099141). The cell culture reagents and other reagents were purchased from Sigma.

Cultured Neonatal Rat Cardiomyocytes and Infection With Recombinant Adenoviral Vectors

Primary neonatal rat cardiomyocytes (NRCMs) were isolated from the hearts of 1- to 2-day-old Sprague-Dawley rats as previously described.[2,18–20] The NRCMs were seeded at a density of 2×10^5 cells per well onto 6-well culture plates coated with gelatin. Then, the cells were cultured in plating medium consisting of DMEM/F12 (C11330, Gibco) medium supplemented with 10% fetal bovine serum, BrdU (0.1 mmol/L, to inhibit the proliferation of fibroblasts) and penicillin/streptomycin. After 48 hours, the cells were maintained in serum-free DMEM/F12 for 12 hours before stimulation with 1 μmol/L Ang II or PBS for another 24 or 48 hours. To silence PHLDA3 expression, an adenovirus harboring PHLDA3 short hairpin RNA (shPHLDA3) was constructed. AdshRNA was used as a control. To overexpress PHLDA3, cDNA containing the entire coding region of human PHLDA3 under the control of the cytomegalovirus promoter was inserted into replication-defective adenoviral vectors (AdPHLDA3). Meanwhile, an adenoviral vector encoding the green fluorescent protein (AdGFP) gene served as a control. The NRCMs were infected with the indicated adenovirus as described above at a multiplicity of infection of 100 for 24 hours before use in

subsequent experiments. For AKT inhibitor experiment, after 48 hours of cultivation, the cells were serum-deprived for another 12 hours and then treated with Ang II and/or the AKT inhibitor MK-2206 (Selleckchem, S1078, 1 μmol/L).

Immunofluorescence Analysis

To assess the cell surface area of NRCMs, immunofluorescence staining was performed. After the abovementioned treatments, the NRCMs were fixed in 3.7% formaldehyde, permeabilized with 0.2% Triton X-100 in PBS, and incubated with a primary antibody against α-actinin (05-384 Merck Millipore, 1:100 dilution) following standard immunofluorescence staining techniques. The cell sizes were analyzed and measured by Image-Pro Plus 6.0 software.

Animals

All animal protocols were reviewed and approved by the Animal Care and Use Committee of First Hospital of Jilin University.

Generation of cardiac-specific PHLDA3 knockout mice

PHLDA3$^{loxP/loxP}$ (PHLDA3-Flox) mice were generated using the CRISPR/Cas9 system to insert 2 LoxP sequences flanking the first exon of PHLDA3. Two single-guide RNAs targeting 2 locations of PHLDA3 were designed using an online CRISPR design tool (http:// tools.genome-engineering.org). The donor plasmid containing exon 1 flanked by 2 loxP sites and the 2 homologous arms were used as the template to repair the double-strand breaks generated by homologous recombination. One-cell-stage embryos were created from zygotes injected with the donor vector, sgRNA1 & sgRNA2 and Cas9 mRNAs. Homozygous PHLDA3-Flox mice were established by the obtained mice with exon 1 flanked by 2 loxP sites on one allele. Then, the PHLDA3$^{loxP/loxP}$ mice were crossed with α-MHC-MerCreMer (Jackson Laboratory, stock No. 005650) transgenic mice to produce PHLDA3$^{loxP/loxP}$/α-MHC-MCM mice. The cardiomyocyte-specific conditional PHLDA3 knockout (PHLDA3-CKO) mice were induced by injecting 6-week-old PHLDA3$^{loxP/loxP}$/α-MHC-MCM mice with tamoxifen (Sigma-Aldrich, T5648, 25 mg/kg per day) for 5 consecutive days. The α-MHC-MCM mice and PHLDA3-Flox mice were also treated with an equal dose of tamoxifen as controls.

Generation of cardiac-specific PHLDA3 transgenic mice

To generate conditional PHLDA3 transgenic (TG) mice, CAG-loxP-CAT-loxP-PHLDA3 constructs were generated and microinjected into fertilized C57BL/6 embryos. To identify the obtained mice, we used polymerase chain reaction (PCR) to analyze tail genomic DNA. The primers used for identification are as follows: 5′-CATGTCTGGATCGATCCCCG-3′ and 5′-TTAGGACACAAGGGTCCCAG-3′. The CAG-loxP-CAT-loxP-PHLDA3-TG mice were then breed with α-MHC-MCM mice to generate CAG-CAT-PHLDA3/α-MHC-MCM mice. To generate cardiac-specific PHLDA3-overexpressing mice, 6-week-old CAG-CAT-PHLDA3/α-MHC-MCM mice were intraperitoneally injected with tamoxifen for 5 consecutive days. Mice with cardiomyocyte-specific PHLDA3 overexpression were designated PHLDA3-TG mice. The α-MHC-MCM mice that underwent the same treatment with tamoxifen served as non-transgenic (NTG) controls.

Mouse Grouping

Mouse models were divided into 10 groups: α-MHC-MCM sham (n=13), PHLDA3-Flox sham (n=12), PHLDA3-CKO sham (n=12), α-MHC-MCM AB (n=14), PHLDA3-Flox AB (n=14), PHLDA3-CKO AB (n=13), NTG sham (n=12), TG sham (n=13), NTG AB (n=13), TG AB (n=13).

Aortic Banding in Animals

The models of pressure overload-induced cardiac hypertrophy were generated by using aortic banding (AB), as previously described.[2,18–20] Male mice aged 8 to 10 weeks (weighing 24–27 g) were subjected to an AB procedure. Briefly, after anesthetization with sodium pentobarbital via an intraperitoneal injection and confirmation of the lack of a toe pinch reflex, the left chest of each mouse was opened to visualize the thoracic aorta at the second intercostal space. AB was achieved by ligating the thoracic aorta against a 26/27-gauge needle with a 7-0 silk suture. After ligation, the needle was removed swiftly before closing the thoracic cavity. Then, Doppler analysis was used to ensure that the aorta was constricted. The sham-operated mice were subjected to a similar procedure without aortic constriction.

Exercise Protocols

To induce physiological cardiac hypertrophy and remodeling, the mice were subjected to swimming training in accordance to the protocol described.[21] In brief, during the first 8 days, forced swimming was performed in 8- to 10-week old mice for 10 minutes twice per day, with an increment of 10 minutes each day until 2 sessions of 90 minutes were achieved on the ninth day. Thereafter, all training mice swam for 14 additional days (22 days total) by 2 daily swimming sessions of 90 minutes. During swimming, the mice were continuously monitored to avoid submerging under the water surface and to ensure equal exertion. On the 23rd day, mice were euthanized for further analyses.

Echocardiographic Measurements

After anesthetization with 2% inhaled isoflurane, the cardiac structure and function of the mice were measured

at the indicated time point using a Mylab 30CV machine (ESAOTE) with a 15-MHz transducer. To measure the left ventricular (LV) end-diastolic diameter (LVEDd) and LV end-systolic diameter (LVESd), the LV was imaged in M-mode with a sweep speed of 50 mm/s at the level of the midpapillary muscle. The LV fractional shortening (LVFS) was calculated with the formula: (LVEDd−LVESd)/LVEDd×100.

Histological Analyses

Hearts were harvested and then arrested in diastole with 10% potassium chloride solution. Then, the hearts were fixed in 10% formalin, dehydrated and embedded in paraffin. Subsequently, 5-μm-thick sections of the hearts were obtained from the midpapillary muscle level and stained with hematoxylin and eosin and picrosirius red to assess the histopathology and collagen deposition. Images of cardiomyocytes and collagen deposition were captured by microscopy to measure the cross-sectional area of cardiomyocytes and collagen volume using a quantitative digital analysis imaging system (Image-Pro Plus 6.0).

Real-Time PCR and Western Blotting

For real-time PCR, total mRNA from cultured primary NRCMs or frozen mouse ventricular tissues was extracted using TRIzol reagent (15596-026, Invitrogen). Then, the RNA samples were reverse-transcribed into cDNA by using the Transcriptor First Strand cDNA Synthesis Kit (04896866001, Roche). To avoid DNA contamination effectively, the primer design of Real-Time PCR was to cross the exons. Real-time PCR was used by applying SYBR Green (04887352001, Roche), and the results were normalized to the corresponding GAPDH gene expression level.

For Western blotting, total proteins from the NRCMs or the left ventricular tissues were first lysed in RIPA lysis buffer (720 μL of RIPA, 20 μL of phenylmethyl sulfonyl fluoride, 100 μL of complete protease inhibitor cocktail, 100 μL of Phos-stop, 50 μL of NaF, and 10 μL of Na_3VO_4), and the protein concentrations were measured with a BCA protein assay kit (Pierce). Protein (50 μg) was separated by SDS-PAGE (Invitrogen) and transferred to a polyvinylidene difluoride membrane (Millipore). After blocking with 5% non-fat milk at room temperature for 1 hour, the membranes were incubated with different primary antibodies at 4°C overnight. After incubation with peroxidase-conjugated secondary antibodies at room temperature for 1 hour, the membranes were reacted with ECL reagents before visualization using the Bio-Rad ChemiDoc XRS$^+$ system. The expression levels of specific proteins were normalized to the corresponding GAPDH expression level.

In Vivo Inhibition Experiment With LY294002

LY294002, a PI3K/AKT inhibitor, was purchased from Sigma (L9908) and dissolved in dimethyl sulfoxide (DMSO). Then, the mixture was administered by intraperitoneal injection at a dose of 50 mg/kg daily for 4 weeks following AB. The control group was given an equal volume of DMSO without LY294002.

Statistical Analysis

Statistical analyses were performed using the SPSS software for Windows (version 21.0, IBM Corp.). The Shapiro-Wilk test was applied for normality and the data of each group were in normal distribution. The Levene Test was used for the test for homogeneity of variance. The 2-tailed Student *t* test was used to analyze the differences between 2 groups, whereas one-way ANOVA was applied for multiple comparisons with Bonferroni post hoc analysis for data meeting homogeneity of variance or with Tamhane T2 analysis for data of heteroscedasticity. The results are presented as the mean±SD. $P<0.05$ was considered to be significant.

Results

PHLDA3 Expression is Decreased in Hypertrophic Hearts and Cardiomyocytes

To investigate the potential role of PHLDA3 in the progression of pathological cardiac hypertrophy and heart failure, we first measured the expression levels of PHLDA3 in hypertrophic mouse hearts by Western blotting. The results showed that PHLDA3 protein expression levels were progressively decreased in mice at 4 and 8 weeks after aortic banding (AB) compared with those in mice after the sham operation, accompanied by increased levels of atrial natriuretic peptide, a hypertrophic marker (Figure 1A). Consistently, similar trends in PHLDA3 levels were also confirmed in neonatal rat cardiomyocytes (NRCMs) stimulated with angiotensin II (Ang II) for 24 and 48 hours when compared with PBS-treated groups (Figure 1B). Taken together, these findings suggest that PHLDA3 may be involved in the development of pathological cardiac hypertrophy and heart failure.

PHLDA3 Inhibits Ang II-Induced Cardiomyocyte Hypertrophy In Vitro

To validate this hypothesis, gain- and loss-of-function studies were performed in cardiomyocytes by infecting NRCMs with adenovirus harboring PHLDA3 short hairpin RNA (AdshPHLDA3), AdshRNA, PHLDA3 cDNA (AdPHLDA3), and AdGFP (Figure 2A). Subsequently, the cells were exposed to

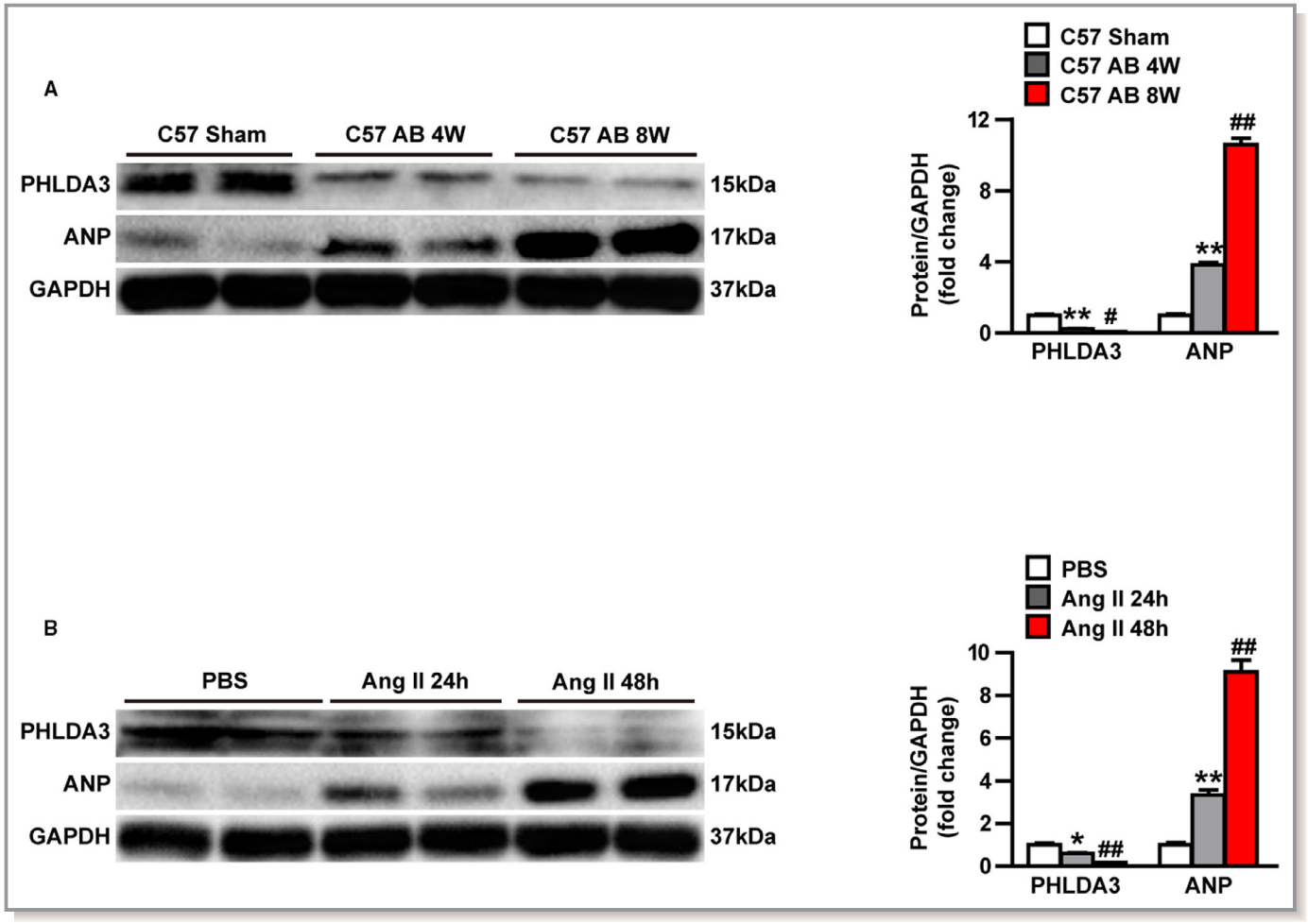

Figure 1. PHLDA3 expression is reduced in the development of pathological cardiac hypertrophy and heart failure. **A**, Representative Western blots and quantitative analysis of PHLDA3 and ANP protein levels in heart tissues from C57BL/6J mice subjected to sham or AB surgery at the indicated time points (n=6 per group). **B**, Representative Western blots and quantitative analysis of PHLDA3 and ANP protein levels in cultured neonatal rat cardiomyocytes incubated with PBS or Ang II at the indicated time points (n=3 independent experiments). $^{*}P<0.05$ or $^{**}P<0.01$ vs sham or PBS; $^{\#}P<0.05$ or $^{\#\#}P<0.01$ vs AB 4w or Ang II 24 hours. By Tamhane's T2 analysis (**A** and **B**). AB indicates aortic banding; Ang II, angiotensin II; ANP, atrial natriuretic peptide; PHLDA3, pleckstrin homology-like domain family A, member 3.

either Ang II (1 μmol/L) or PBS for 48 hours and immunostained with α-actinin to determine the cell surface area. The results showed that there were no significant changes in cardiomyocyte morphology or cell surface area among PBS-treated NRCMs (Figure 2B through 2D). However, in response to Ang II stimulation, the cross-sectional areas were significantly augmented in the AdshPHLDA3 groups compared with the AdshRNA groups but remarkably reduced in the AdPHLDA3 groups compared with the AdGFP groups (Figure 2B through 2D). Next, hypertrophic hallmarks, such as *Anp* and *Myh7*, were determined by real-time polymerase chain reaction. In accordance with the variation tendency of cell surface area, these hypertrophic markers were markedly increased in the AdshPHLDA3 groups after Ang II treatment, whereas they were markedly suppressed in the AdPHLDA3 groups compared with their controls (Figure 2E and 2F). Thus, these in vitro data implicate PHLDA3 as a negative regulator of Ang II-induced cardiomyocyte hypertrophy.

Cardiomyocyte-Specific Knockout of PHLDA3 Aggravates Pressure Overload-Induced Pathological Cardiac Hypertrophy

Given that the development and mechanism of pressure overload-induced pathological cardiac hypertrophy in vivo are more complicated than those of Ang II-induced cardiomyocyte hypertrophy in vitro, we next sought to use a tamoxifen-inducible α-MHC-Cre system to generate cardiomyocyte-specific conditional PHLDA3 knockout mice (PHLDA3-CKO) to verify the results in vitro. The absence of PHLDA3 in the mouse hearts was confirmed by Western blotting (Figure 3A and 3B). Notably, compared with the α-MHC-MCM or

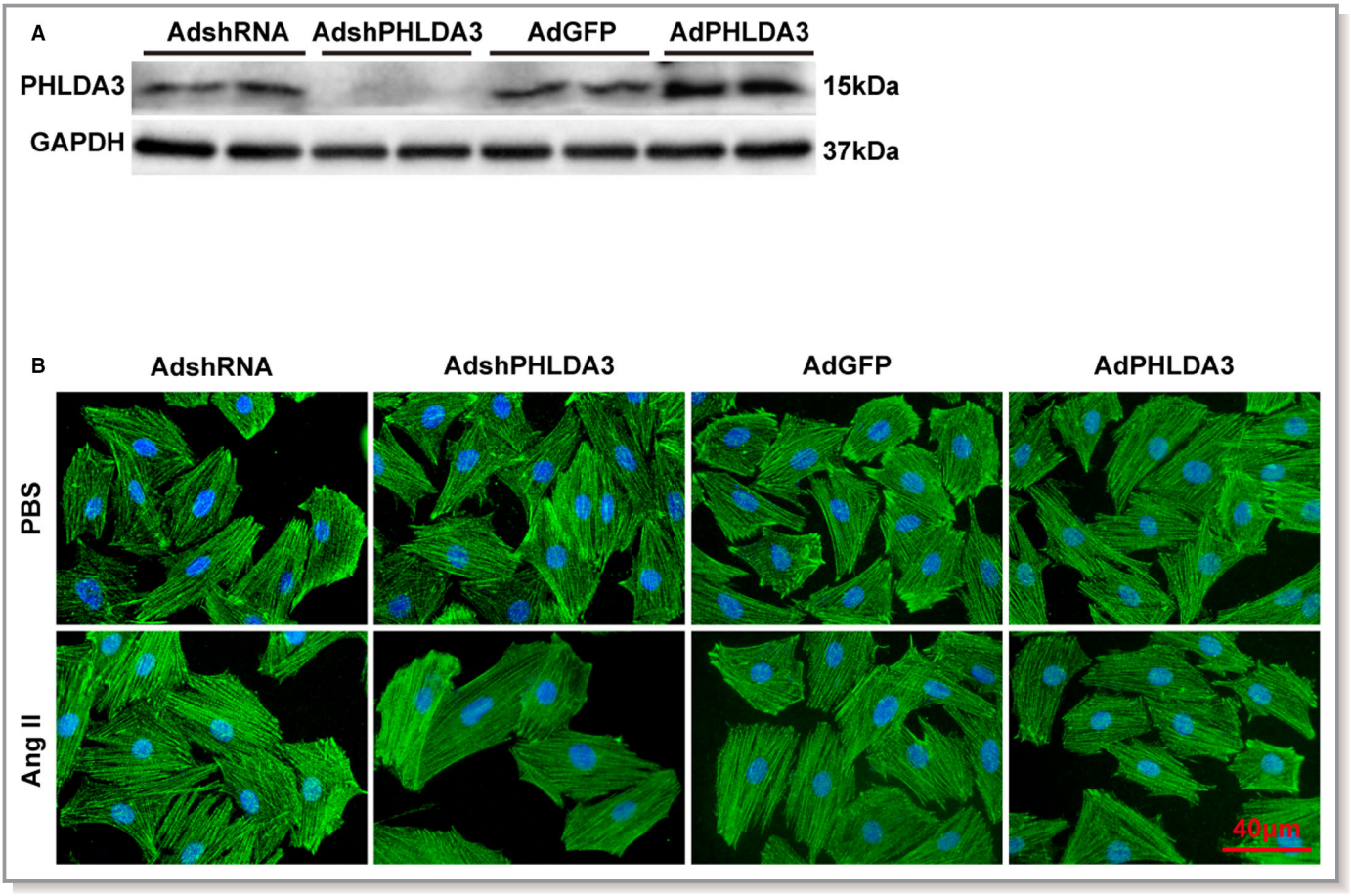

Figure 2. PHLDA3 attenuates Ang II-induced cardiomyocyte hypertrophy in vitro. **A**, Representative Western blots verify PHLDA3 expression in cultured neonatal rat cardiomyocytes (NRCMs) infected with AdshRNA, AdshPHLDA3, AdGFP and AdPHLDA3. **B**, Representative immunofluorescence images of NRCMs infected with AdshRNA, AdshPHLDA3, AdGFP and AdPHLDA3 after treatment with PBS or Ang II for 48 hours (green: α-actinin; blue: nuclear; scale bar, 40 μm). **C**, Quantitative results of the cell surface area of NRCMs infected with AdshRNA or AdshPHLDA3 after treatment with PBS or Ang II for 48 hours. **D**, Quantitative results of the cell surface area of NRCMs infected with AdGFP or AdPHLDA3 after treatment with PBS or Ang II for 48 hours. **E**, Transcript levels of the hypertrophic biomarkers *Anp* and *Myh7* in NRCMs infected with AdshRNA or AdshPHLDA3. **F**, Transcript levels of the hypertrophic biomarkers *Anp* and *Myh7* in NRCMs infected with AdGFP or AdPHLDA3. $^{**}P<0.01$ vs AdshRNA+PBS, $^{\#\#}P<0.01$ vs AdshRNA+Ang II in (**C** and **E**); $^{**}P<0.01$ vs AdGFP+PBS, $^{\#}P<0.05$ or $^{\#\#}P<0.01$ vs AdGFP+Ang II in (**D** and **F**). n=3 independent experiments in (**A** through **F**). n>50 cells per group in (**C** and **D**). By Tamhane T2 analysis (**C**, **E** [*Myh7*] and **F**) or Bonferroni post hoc analysis (**D** and **E** [*Anp*]). AdGFP indicates adenoviral green fluorescent protein; AdPHLDA3, adenoviral vectors containing the PHLDA3 cDNA; AdshPHLDA3, adenoviral vectors harboring the PHLDA3 short hairpin RNA; AdshRNA, adenoviral short hairpin RNA; Ang II, angiotensin II; *Anp*, atrial natriuretic peptide; *Myh7*, myosin heavy chain 7; PHLDA3, pleckstrin homology-like domain family A, member 3.

PHLDA3-Flox control groups, the PHLDA3-CKO mice were normal and fertile and had no apparent abnormalities in cardiac morphology and function at baseline (Figure 3C through 3J). These mice subsequently underwent AB or sham surgery and were evaluated after 4 weeks. As expected, the results showed that the hallmarks of the hypertrophic response, the ratios of heart weight/body weight (HW/BW), lung weight/BW (LW/BW) and HW/tibia length (HW/TL), were significantly increased compared with those in the sham group (Figure 3C through 3E). Notably, these hypertrophic indices were further increased in PHLDA3-CKO mice compared with the α-MHC-MCM or PHLDA3-Flox mice after AB surgery (Figure 3C through 3E). Histopathologically, a thicker ventricular wall and greater cardiomyocyte cross-sectional area were observed in PHLDA3-CKO mice than in control mice after AB, as shown via hematoxylin and eosin staining (Figure 3F and 3G). In line with the gross pathological results, echocardiography measurements indicated that cardiac hypertrophy and function were worse in the PHLDA3-CKO mice than in the controls, as evidenced by a larger left ventricular end-diastolic diameter (LVEDd), left ventricular end-systolic diameter (LVESd), left ventricular posterior wall thickness at end diastole (LVPWd) and left ventricular posterior wall thickness at end systole (LVPWs) but a lower fractional shortening (FS%) (Figure 3H through 3J, Figure S1A through S1C). Furthermore, picrosirius red staining revealed

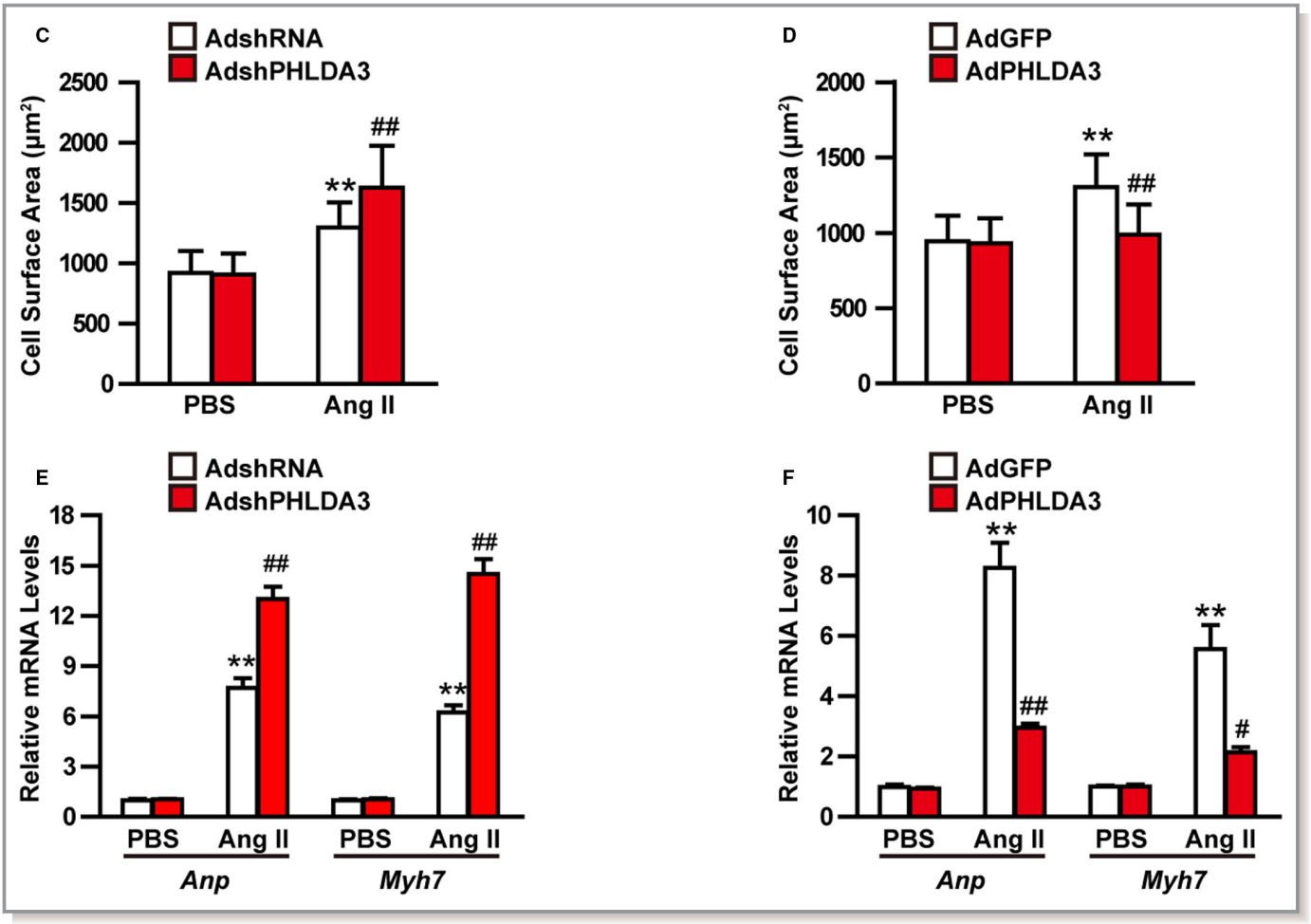

Figure 2. Continued.

that cardiac fibrosis induced by AB, including perivascular and interstitial fibrosis, was more severe in PHLDA3-CKO mice than in controls (Figure 3K and 3L). Consistently, the expression levels of hypertrophic and fibrotic markers, including *Anp*, brain natriuretic peptide (*Bnp*), myosin heavy chain 7 (*Myh7*), *collagen Iα*, *collagen III*, and connective tissue growth factor (*Ctgf*), were dramatically elevated in the PHLDA3-CKO mice compared with the controls (Figure 3M and 3N). Overall, these data illustrate that the absence of PHLDA3 in the heart exacerbated pressure overload-induced cardiac hypertrophy and fibrosis.

Besides, we also detected the role of PHLDA3 on physiological cardiac hypertrophy induced by exercise training. The results showed that the ratio of HW/BW and the cardiomyocyte cross-sectional area were remarkably increased in the exercise group compared with sedentary controls without fibrosis (Figure S2). However, the PHLDA3 deficiency has no significant regulatory effect on physiological myocardial hypertrophy (Figure S2). Therefore, our present study focused on the effect of PHLDA3 on pathological cardiac hypertrophy.

Overexpression of PHLDA3 Mitigates AB-Induced Cardiac Remodeling

To further confirm the ameliorative effect of PHLDA3 on the development of pathological cardiac hypertrophy in vivo, cardiomyocyte-specific PHLDA3-overexpressing transgenic mice (*PHLDA3*-TG) were generated, and 4 independent lines of PHLDA3-TG mice were established and verified by Western blotting (Figure 4A and 4B). At baseline, PHLDA3-TG mice exhibited no apparent morphological or pathological cardiac abnormalities (Figure 4C through 4J). Predictably, cardiomyocyte-specific PHLDA3 overexpression displayed a notable alleviation of cardiac hypertrophy compared with the non-transgenic (NTG) controls at 4 weeks after AB operation, as indicated by a reduction in the HW/BW, LW/BW and HW/TL ratios (Figure 4C through 4E). Similarly, hematoxylin and eosin staining revealed that the ventricular cross-sectional area was decreased in AB-induced PHLDA3-TG mice compared with the NTG controls (Figure 4F and 4G). Echocardiographic analysis also showed ameliorated cardiac hypertrophy and improved cardiac function in PHLDA3-TG

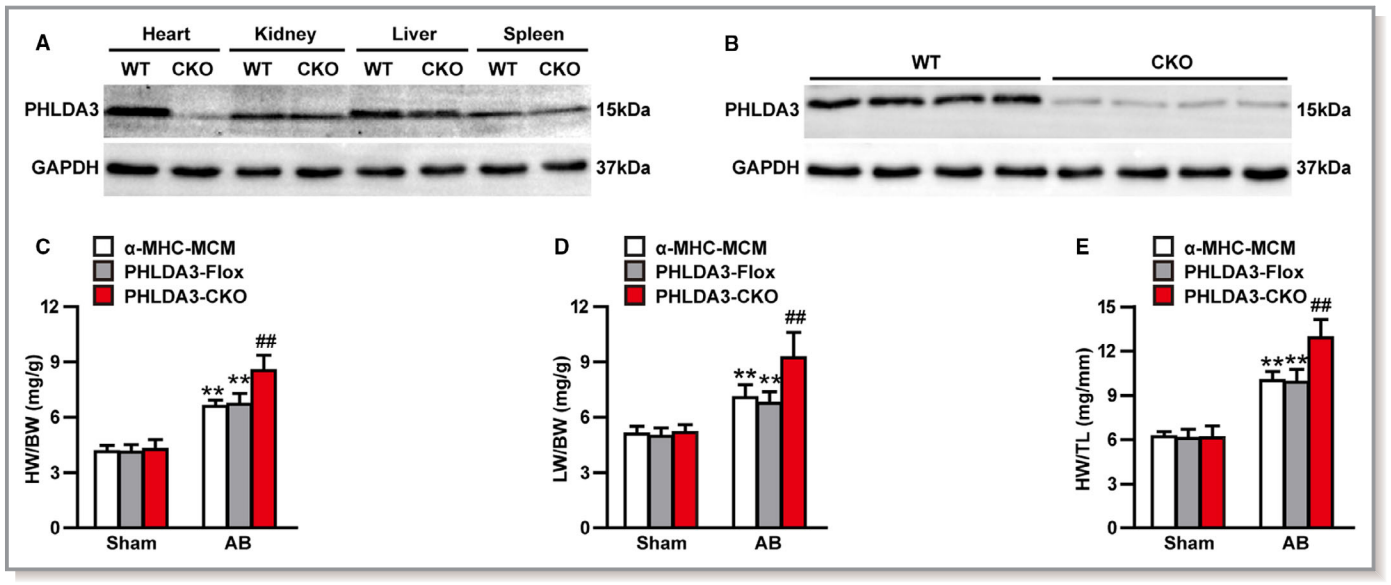

Figure 3. Cardiomyocyte-specific PHLDA3 deficiency accelerates pressure overload-induced pathological cardiac hypertrophy. **A**, Representative Western blots to identify PHLDA3 expression in different organ tissues from PHLDA3-CKO mice and wild-type mice (n=3 independent experiments). **B**, Validation of PHLDA3-CKO mice by Western blotting (n=4 per experimental group). **C** through **E**, Statistical results of the ratios of heart weight/body weight (**C**), lung weight/body weight (**D**), and heart weight/tibia length (**E**) in mice with different genotypes (α-MHC-MCM, PHLDA3-Flox and PHLDA3-CKO) at 4 weeks after sham or aortic banding (AB) surgery (n=12–14 mice per group). **F**, Representative hematoxylin and eosin staining images of the gross morphology and left ventricular muscle of hearts from the indicated groups (n=6–7 mice per group; scale bar, 50 μm). **G**, Statistical results of the cardiomyocyte cross-sectional area from the indicated groups (n>100 cells per group). **H** through **J**, Echocardiographic assessment of the left ventricle end-diastolic diameter (**H**), left ventricle end-systolic diameter (**I**), and fractional shortening (**J**) in the indicated groups at 4 weeks after sham or AB surgery (n=11–14 mice per group). **K**, Representative images of picrosirius red staining of perivascular and myocardial interstitial regions of the hearts from the indicated groups (n=5–7 mice per group; scale bar, 100 μm). **L**, Statistical results of fibrotic areas in the indicated groups (n>30 fields per group). **M** and **N**, Real-time polymerase chain reaction (PCR) showing the mRNA levels of fetal genes (**M**) and fibrotic markers (**N**) in the heart tissues from the indicated groups after 4 weeks of sham or AB surgery (n=4 per group). $*P<0.05$ or $**P<0.01$ vs α-MHC-MCM sham or PHLDA3-Flox sham; $^{\#}P<0.05$ or $^{\#\#}P<0.01$ vs α-MHC-MCM AB or PHLDA3-Flox AB in (**C** through **E**, **G** through **J**, **L** through **N**). By Tamhane T2 analysis (**C** through **E**, **G**, **L** through **N**) or Bonferroni post hoc analysis (**H** through **J**). AB indicates aortic banding; *Anp*, atrial natriuretic peptide; *Bnp*, B-type natriuretic peptide; BW, body weight; CKO, cardiomyocyte-specific conditional PHLDA3 knockout mice; *Ctgf*, connective tissue growth factor; FS, fractional shortening; H&E, hematoxylin and eosin; HW, heart weight; LV, left ventricle; LVEDd, left ventricle end-diastolic diameter; LVESd, left ventricle end-systolic diameter; LW, lung weight; *Myh7*, myosin heavy chain 7; PHLDA3, pleckstrin homology-like domain family A, member 3; TL, tibia length; WT, wild-type mice.

mice (Figure 4H through 4J, Figures S1D through S1F and S3). In addition, the PHLDA3 transgene repressed the development of cardiac fibrosis in both interstitial and perivascular regions (Figure 4K and 4L). Correspondingly, the mRNA levels of cardiac fetal genes and fibrotic markers were markedly decreased in the PHLDA3-TG mice compared with NTG mice (Figure 4M and 4N). To evaluate whether PHLDA3 still has protective effects on intermediate and advanced heart failure, we performed AB and Sham surgery for 8 weeks on PHLDA3-TG mice and the controls. The results showed that PHLDA3 overexpression significantly ameliorated cardiac hypertrophy (Figure S4A through S4E), cardiac dysfunction (Figure S4F through S4I), and cardiac fibrosis (Figure S4J and S4K) induced by AB after 8 weeks. Collectively, these results demonstrate that PHLDA3 overexpression attenuates the development of pathological cardiac hypertrophy and heart failure induced by pressure overload.

PHLDA3 Mediates Cardiac Hypertrophy via Inhibition of the AKT Signaling Pathway

To explore the underlying mechanisms by which PHLDA3 exerts an antihypertrophic effect, we first determined the expression level of the mitogen-activated protein kinases (MAPKs), including MAPK/ERK kinase (MEK) 1/2, extracellular-signal-regulated kinase (ERK) 1/2, c-Jun N-terminal kinase (JNK) 1/2 and P38, which have been proven to be well-accepted, vital players in the progression of pathological cardiac hypertrophy. As shown in Figure 5A and 5B, the members of MAPKs were significantly phosphorylated in AB mice, as expected, compared with the sham controls. However, the phosphorylation of MAPKs in response to pressure overload remained unaltered by both the deficiency and the overexpression of PHLDA3 compared with that in controls. These results unexpectedly showed that the involvement of PHLDA3 in cardiac hypertrophy was independent of the MAPK pathway, which indicates that

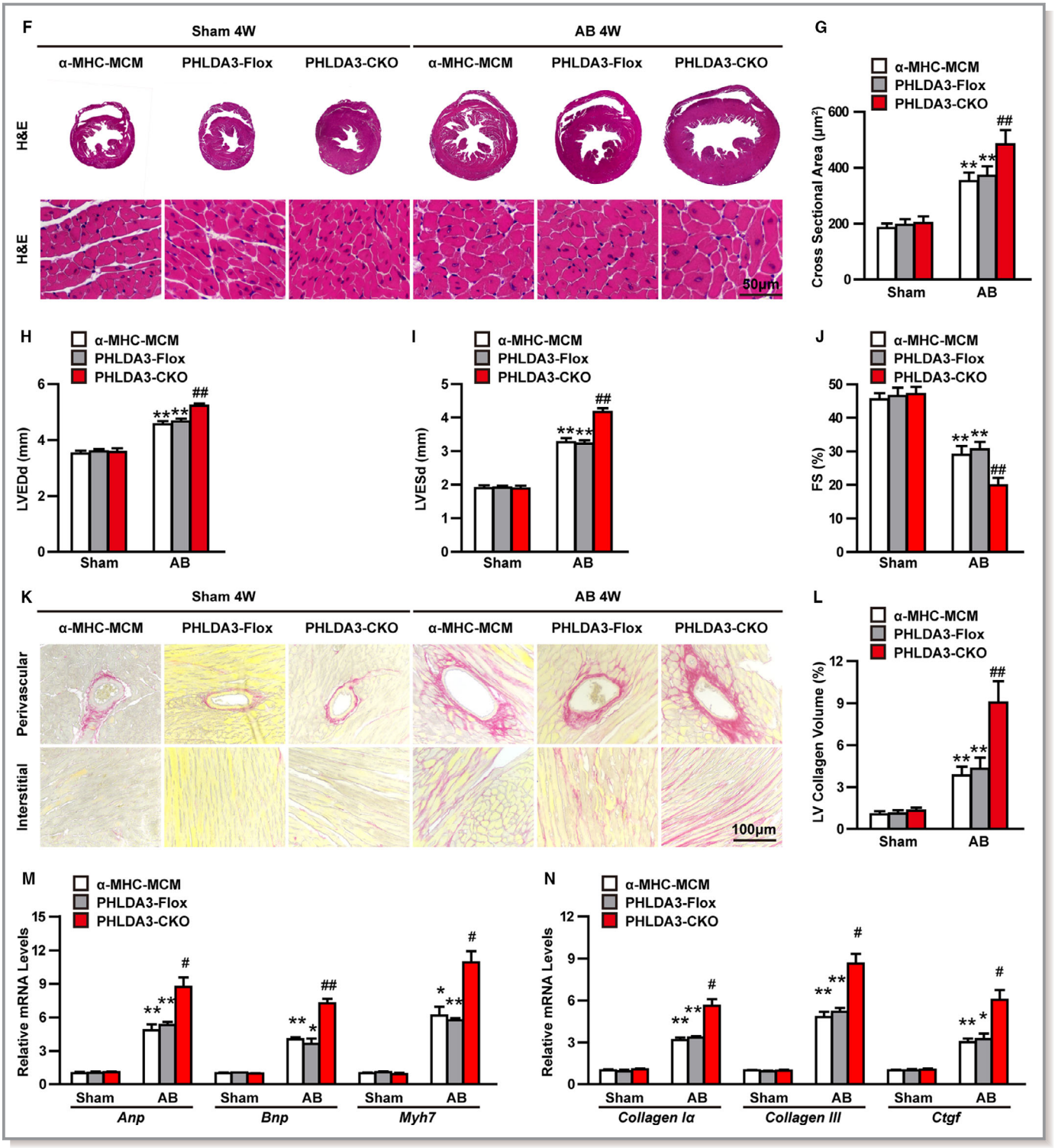

Figure 3. Continued.

there are other mechanisms responsible for PHLDA3-regulated hypertrophic responses. Given the critical role of the AKT pathway in the process of cardiac hypertrophy, we next explored the expression level of AKT signaling components. The results showed that the phosphorylation of AKT, mammalian target of rapamycin (mTOR), glycogen synthase kinase 3β (GSK3β) and ribosomal protein S6 kinase beta-1 (P70S6K) was significantly higher in PHLDA3-CKO mice than in PHLDA3-Flox mice, while PHLDA3 overexpression inhibited the phosphorylation of those proteins in AKT signaling compared with that in NTG controls in response to the induction of hypertrophy (Figure 5C and 5D). To further confirm these findings in vivo,

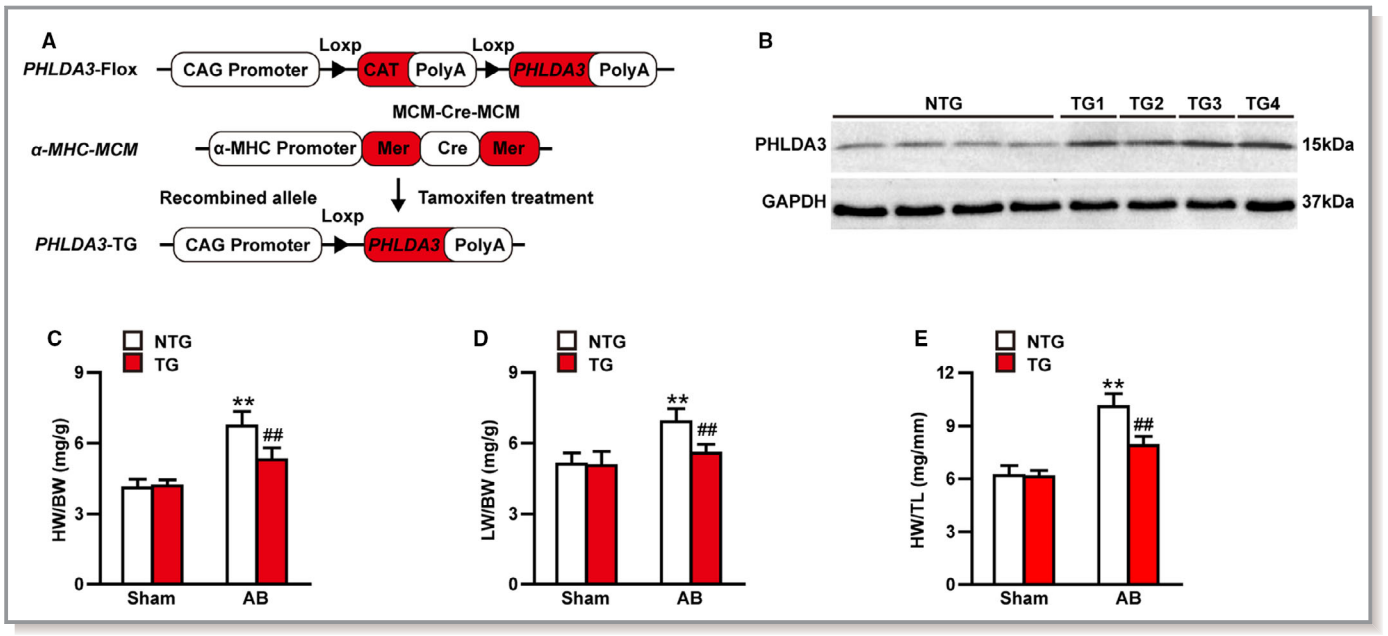

Figure 4. Cardiomyocyte-specific PHLDA3 overexpression blunts the aortic banding (AB)-induced hypertrophic response. **A**, Schematic illustration of the construction of cardiomyocyte-specific PHLDA3 transgenic mouse lines. **B**, Representative Western blots for cardiomyocyte-specific PHLDA3 expression in transgenic mice and their non-transgenic mice controls (n=3 independent experiments). **C** through **E**, Statistical results of the ratios of heart weight/body weight (**C**), lung weight/body weight (**D**), and heart weight/TL (**E**) in non-transgenic mice and transgenic mice at 4 weeks after sham or AB surgery (n=12–13 mice per group). **F**, Representative hematoxylin and eosin staining images of the gross morphology and left ventricular muscle of hearts from the indicated groups (n=6 mice per group; scale bar, 50 μm). **G**, Statistical results of the cardiomyocyte cross-sectional area from the indicated groups (n>100 cells per group). **H** through **J**, Echocardiographic assessment of the left ventricle end-diastolic diameter (**H**), left ventricle end-systolic diameter (**I**), and fractional shortening (**J**) in the indicated groups at 4 weeks after sham or AB surgery (n=11–13 mice per group). **K**, Representative images of picrosirius red staining of perivascular and myocardial interstitial regions of the hearts from the indicated groups (n=6 mice per group; scale bar, 100 μm). **L**, Statistical results of fibrotic areas from the indicated groups (n>30 fields per group). **M** and **N**, Real-time PCR showing the mRNA levels of fetal genes (**M**) and fibrotic markers (**N**) in the heart tissues from the indicated groups at 4 weeks after sham or AB surgery (n=4 per group). $^{**}P<0.01$ vs non-transgenic mice sham; $^{\#\#}P<0.01$ vs non-transgenic mice AB in (**C** through **E**, **G** through **J**, **L** through **N**). By Tamhane T2 analysis (**C**, **E**, **G**, **I**, **L** through **N**) or Bonferroni post hoc analysis (**D**, **H**, and **J**). AB indicates aortic banding; *Anp*, atrial natriuretic peptide; *Bnp*, B-type natriuretic peptide; BW, body weight; *Ctgf*, connective tissue growth factor; FS, fractional shortening; H&E, hematoxylin and eosin; HW, heart weight; LV, left ventricle; LVEDd, left ventricle end-diastolic diameter; LVESd, left ventricle end-systolic diameter; LW, lung weight; *Myh7*, myosin heavy chain 7; NTG, non-transgenic mice; PHLDA3, pleckstrin homology-like domain family A, member 3; TG, conditional PHLDA3 transgenic mice; TL, tibia length.

in vitro NRCMs were infected with adenoviruses as mentioned above and treated with Ang II. Consistent with the in vivo studies, Western blot analysis demonstrated a significant rise in AKT and the phosphorylation of its downstream kinase in the AdshPHLDA3 groups and a remarkable reduction in the AdPHLDA3 groups when compared with the respective control groups (Figure 5E and 5F). Altogether, these results indicate that PHLDA3 may exert its antihypertrophic effect via negative regulation of the AKT-mTOR-GSK3β-P70S6K signaling pathway.

Inhibition of AKT Signaling Reverses the Hypertrophic Phenotype In Vivo and In Vitro

The aforementioned evidence indicated that PHLDA3 attenuates pathological cardiac hypertrophy by inhibiting AKT signaling in the presence of pressure overload and Ang II stimuli. To further determine whether inactivation of AKT could rescue the abnormalities in PHLDA3-CKO mice, we treated PHLDA3-CKO mice and PHLDA3-Flox mice with the PI3K/AKT inhibitor LY294002 or DMSO solution for 4 weeks after AB. As expected, Western blotting revealed that the pressure overload-induced level of AKT phosphorylation was almost completely abrogated in the PI3K/AKTI-treated mice compared with DMSO-treated mice (Figure 6A). PI3K/AKTI treatment remarkably reversed the AB-induced detrimental hypertrophy phenotype, including cardiac and cardiomyocyte hypertrophy, cardiac insufficiency, and cardiac fibrosis in both PHLDA3-CKO and PHLDA3-Flox mice compared with DMSO treatment (Figure 6B through 6K). More importantly, the PI3K/AKT inhibitor LY294002 eliminated the difference between the PHLDA3-CKO and PHLDA3-Flox mice subjected to AB (Figure 6B through 6K). Besides, AKT inhibitor MK-2206 was used to conduct in vitro experiments. The results showed that MK-2206 remarkably reversed the Ang II-induced cardiomyocyte

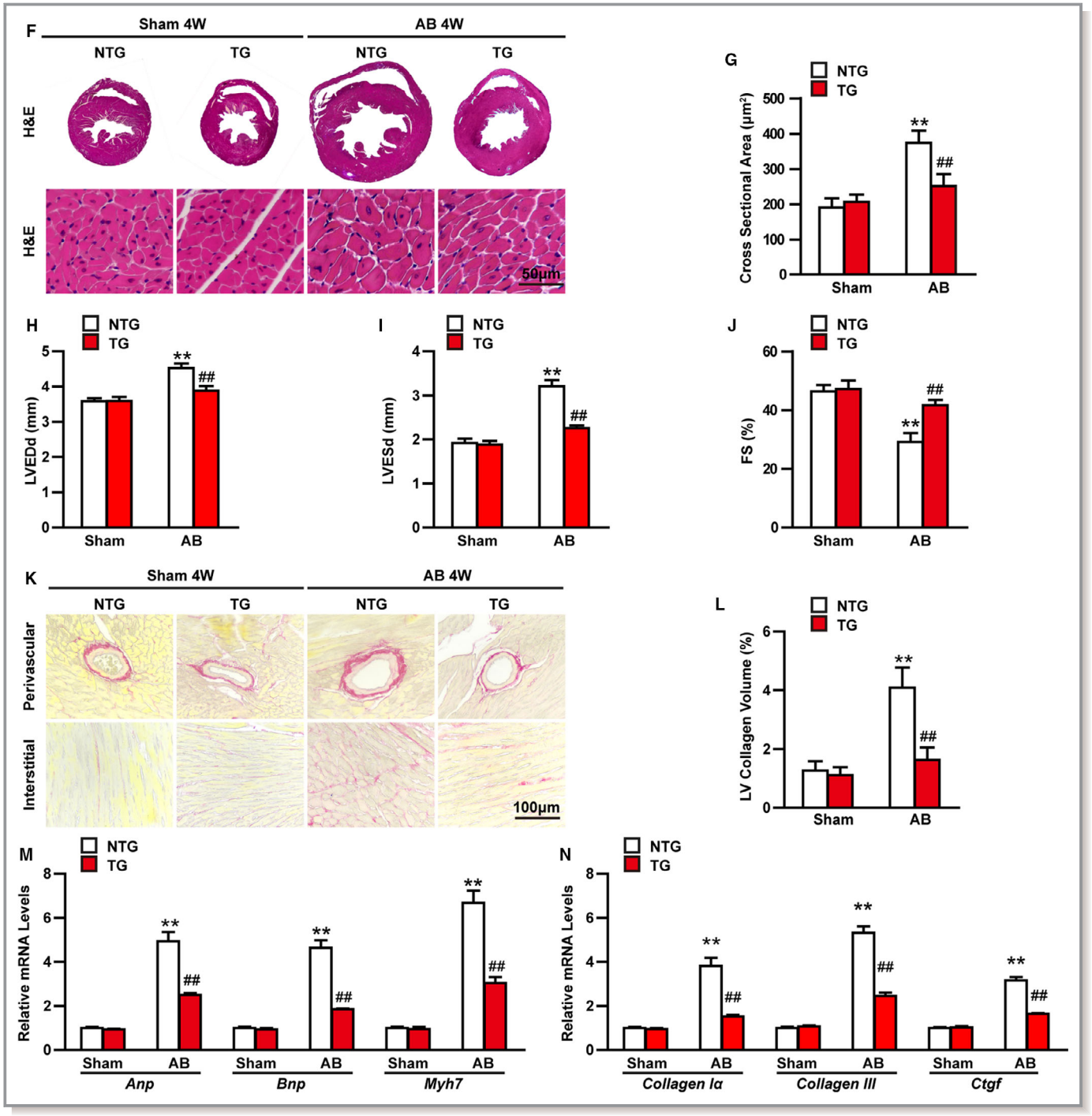

Figure 4. Continued.

hypertrophy phenotype (Figure S5). In summary, these data demonstrate that pharmacological inhibition of AKT rescues the hypertrophic phenotype in vivo and in vitro.

Discussion

Once pathological cardiac hypertrophy progresses into heart failure, the prognosis is often poor, even with the most advanced drug treatment. Therefore, it is of great importance to explore therapeutic targets that can effectively postpone or even reverse the progression of pathological cardiac hypertrophy. Because pathological cardiac hypertrophy is characterized by enlarged cardiomyocytes, interstitial fibrosis and re-expression of fetal gene programs,[22,23] we assessed the role of PHLDA3 in pathological cardiac hypertrophy at gross cardiac, cellular and molecular levels, respectively. The results

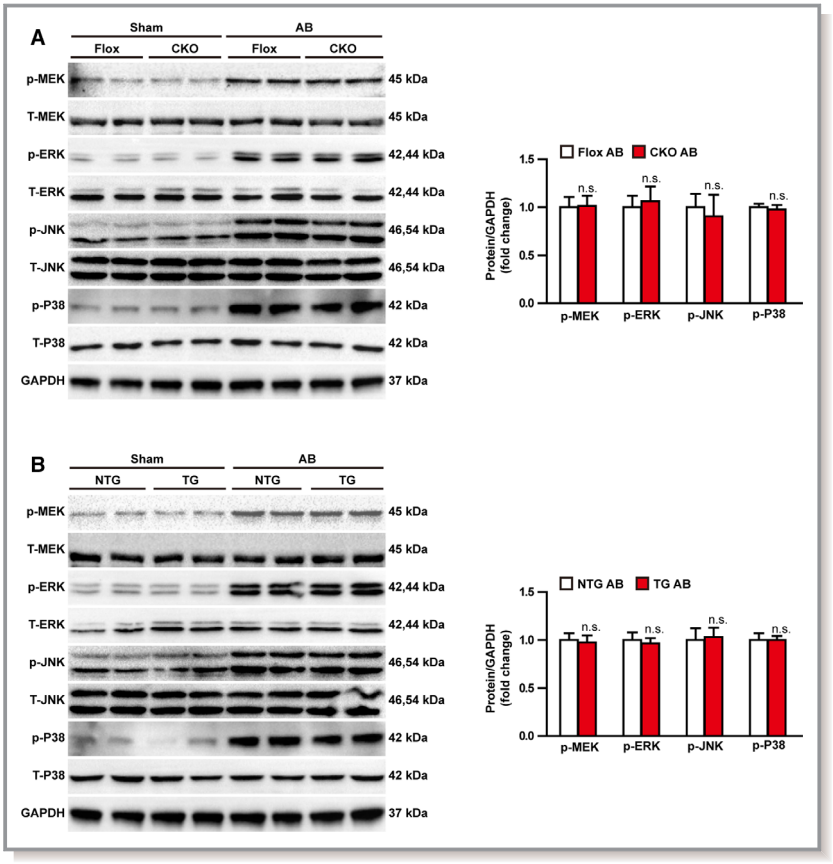

Figure 5. PHLDA3 inhibits the activation of AKT signaling induced by prohypertrophic stimuli. **A** and **B**, Representative Western blots and quantitative analysis of phosphorylated and total MEK1/2, ERK1/2, JNK1/2 and P38 levels in PHLDA3-Flox and PHLDA3-CKO mice (**A**) or transgenic and non-transgenic mice (**B**) at 4 weeks after sham or aortic banding surgery (n=4 mice per group; n.s. means no significant difference vs PHLDA3-Flox aortic banding or non-transgenic mice aortic banding). **C** and **D**, Representative Western blots and quantitative analysis of phosphorylated and total AKT, mTOR, GSK3β, and P70S6K levels in PHLDA3-Flox and PHLDA3-CKO mice (**C**) or transgenic and non-transgenic mice (**D**) at 4 weeks after sham or aortic banding surgery (n=4 mice per group; $^{**}P<0.01$ vs PHLDA3-Flox aortic banding or non-transgenic mice aortic banding). **E** and **F**, Representative Western blots and quantitative analysis of phosphorylated and total AKT, mTOR, GSK3β, and P70S6K levels in neonatal rat cardiomyocytes infected with AdshRNA and AdshPHLDA3 (**E**) or AdGFP and AdPHLDA3 (**F**) and treated with PBS or Ang II (n=3 independent experiments; $^{**}P<0.01$ vs AdshRNA+Ang II or AdGFP+Ang II). By 2-tailed Student *t*-test (**A** through **C** [p-AKT], **C** [p-GSK3β], **C** [p-P70S6K], **D** [p-mTOR], **F** [p-mTOR]) or Welch test (**C** [p-mTOR], **D** [p-AKT], **D** [p-GSK3β], **D** [p-P70S6K], **E** and **F** [p-AKT], **F** [p-GSK3β], **F** [p-P70S6K]). AB indicates aortic banding; AdGFP, adenoviral green fluorescent protein; AdPHLDA3, adenoviral vectors containing the PHLDA3 cDNA; AdshPHLDA3, adenoviral vectors harboring the PHLDA3 short hairpin RNA; AdshRNA, adenoviral short hairpin RNA; Ang II, angiotensin II; CKO, cardiomyocyte-specific conditional PHLDA3 knockout mice; ERK, extracellular regulated protein kinase; Flox, PHLDA3$^{loxP/loxP}$ (PHLDA3-Flox) mice; GSK3β, glycogen synthase kinase 3β; JNK, c-Jun N-terminal kinase; MEK, MAPK/ERK kinase; mTOR, mammalian target of rapamycin; NTG, non-transgenic mice; p38, protein 38; P70S6K, ribosomal protein S6 kinase beta-1; PHLDA3, pleckstrin homology-like domain family A, member 3; TG, conditional PHLDA3 transgenic mice.

consistently showed that cardiomyocyte-specific loss of PHLDA3 promoted the cardiomyocyte hypertrophic response, whereas cardiac-specific overexpression of PHLDA3 significantly protected against these maladaptive pathological consequences by using gain and loss-of-function approaches in vitro and in vivo. Different degrees of interstitial fibrosis occurred in

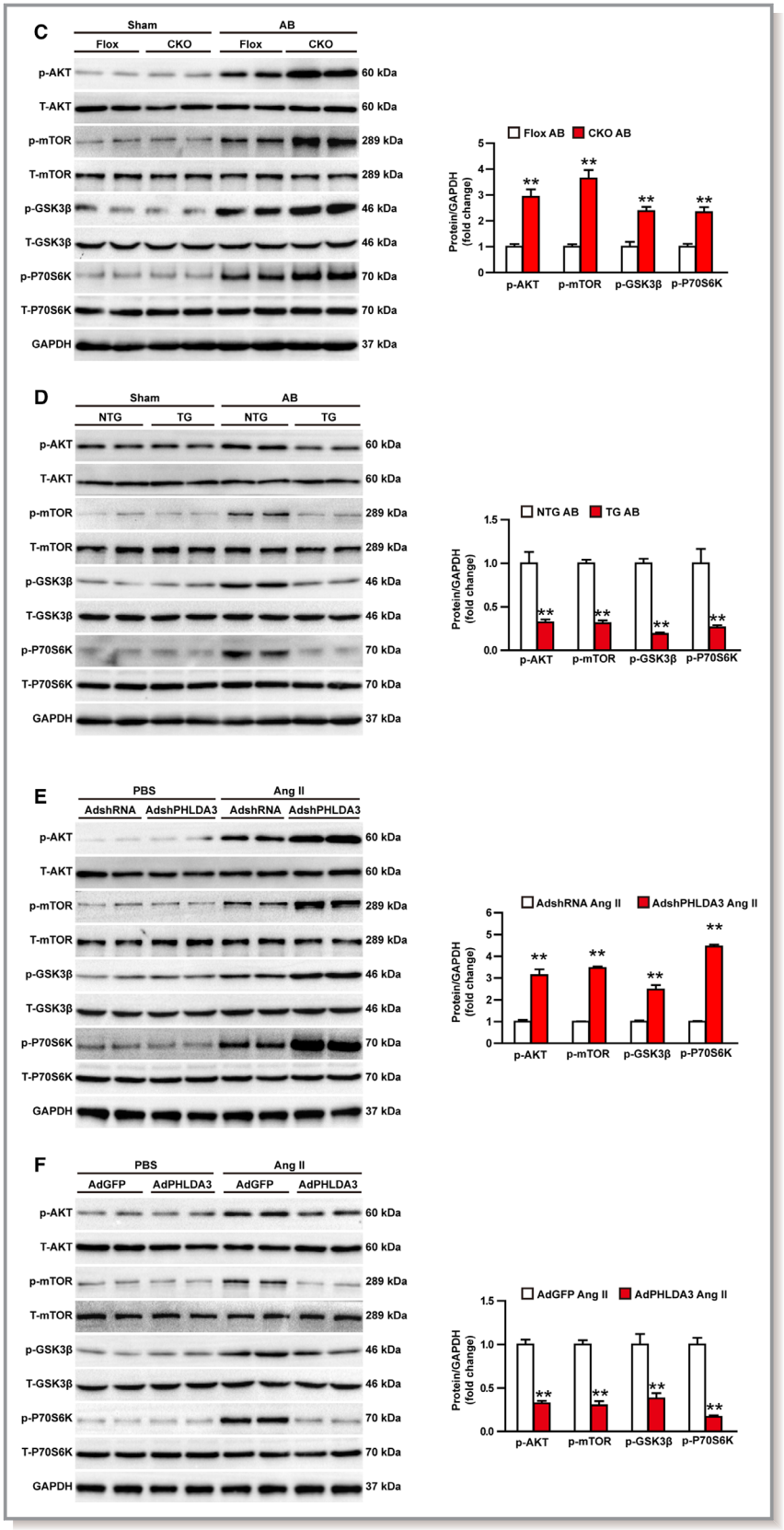

Figure 5. Continued

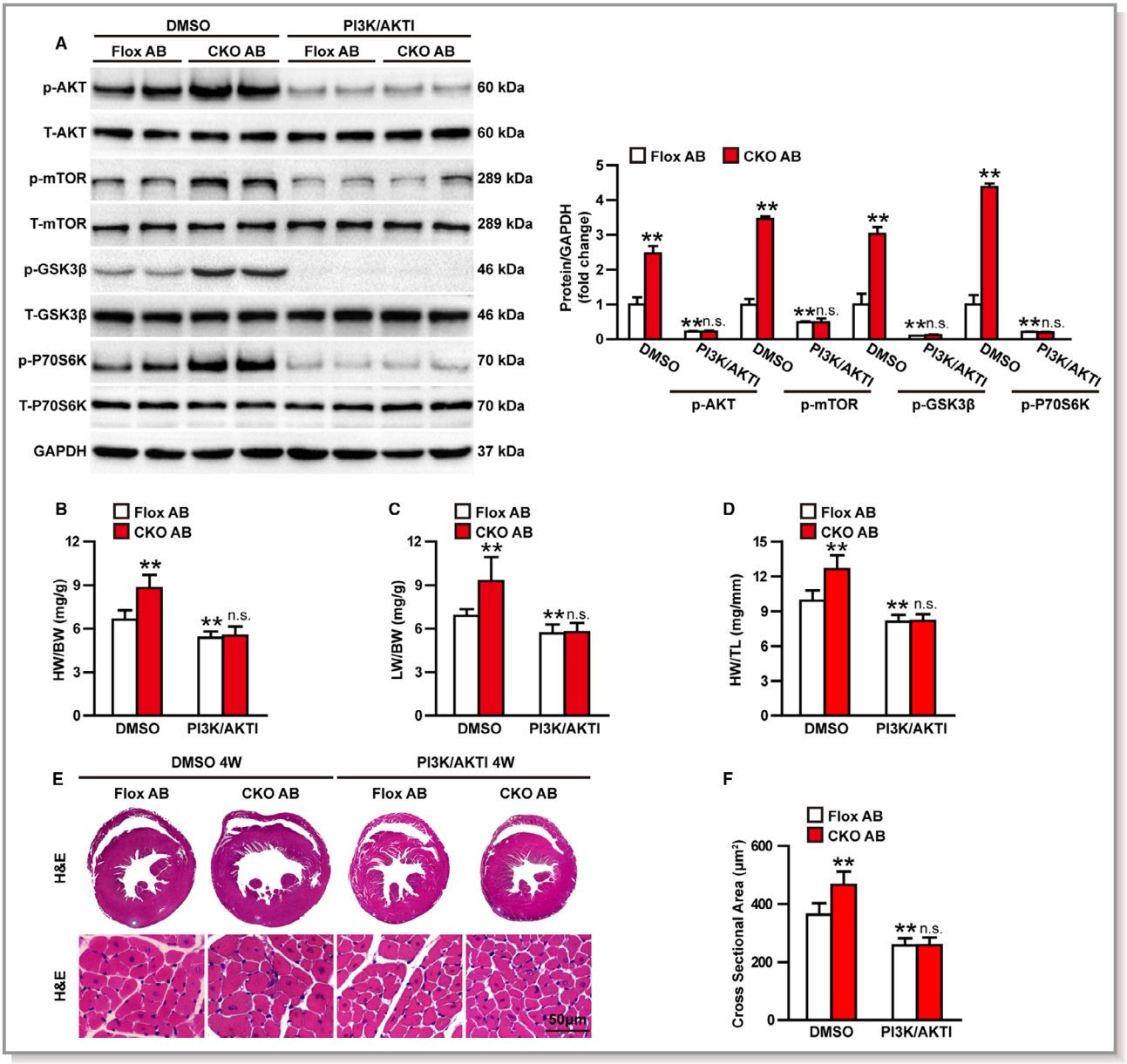

Figure 6. Blockage of AKT signaling reverses the PHLDA3-CKO-induced pathological cardiac hypertrophy phenotype. **A**, Representative Western blots and quantitative analysis of phosphorylated and total AKT, mTOR, GSK3β, and P70S6K levels in PHLDA3-Flox and PHLDA3-CKO mice treated with DMSO or PI3K/AKTI (LY294002) at 4 weeks after AB surgery (n=4 mice per group). **B** through **D**, Statistical results of the ratios of heart weight/body weight (**B**), lung weight/body weight (**C**), and heart weight/tibia length (**D**) in mice with different genotypes (PHLDA3-Flox and PHLDA3-CKO) treated with DMSO or PI3K/AKTI at 4 weeks after aortic banding surgery (n=12–14 mice per group). **E**, Representative images of hematoxylin and eosin staining of the gross morphology and left ventricular muscle of hearts from the indicated groups (n=6 mice per group; scale bar, 50 μm). **F**, Statistical results of the cardiomyocyte cross-sectional area in the indicated groups (n>100 cells per group). **G** through **I**, Echocardiographic assessment of the left ventricle end-diastolic diameter (**G**), left ventricle end-systolic diameter (**H**), and fractional shortening (**I**) in the indicated groups at 4 weeks after aortic banding surgery (n=11–13 mice per group). **J**, Representative images of picrosirius red staining of perivascular and myocardial interstitial regions of hearts from the indicated groups (n=6 mice per group; scale bar, 100 μm). **K**, Statistical results of fibrotic areas from the indicated groups (n>30 fields per group). ***P*<0.01 vs PHLDA3-Flox DMSO+AB; n.s. indicates no significant difference in (**A** through **D**, **F** through **I**, and **K**). By Bonferroni post hoc analysis (**A** [p-mTOR], **B**, and **G** through **I**) or Tamhane T2 analysis (**A** [p-AKT], **A** [p-GSK3β], **A** [p-P70S6K], **C**, **D**, **F** and **K**). AB indicates aortic banding; BW, body weight; CKO, cardiomyocyte-specific conditional PHLDA3 knockout mice; DMSO, dimethyl sulfoxide; Flox, PHLDA3$^{loxP/loxP}$ (PHLDA3-Flox) mice; FS, fractional shortening; GSK3β, glycogen synthase kinase 3β; H&E, hematoxylin and eosin; HW, heart weight; LV, left ventricle; LVEDd, left ventricle end-diastolic diameter; LVESd, left ventricle end-systolic diameter; LW, lung weight; mTOR, mammalian target of rapamycin; P70S6K, ribosomal protein S6 kinase beta-1; PI3K/AKTI, PI3K/AKT inhibitor; TL, tibia length.

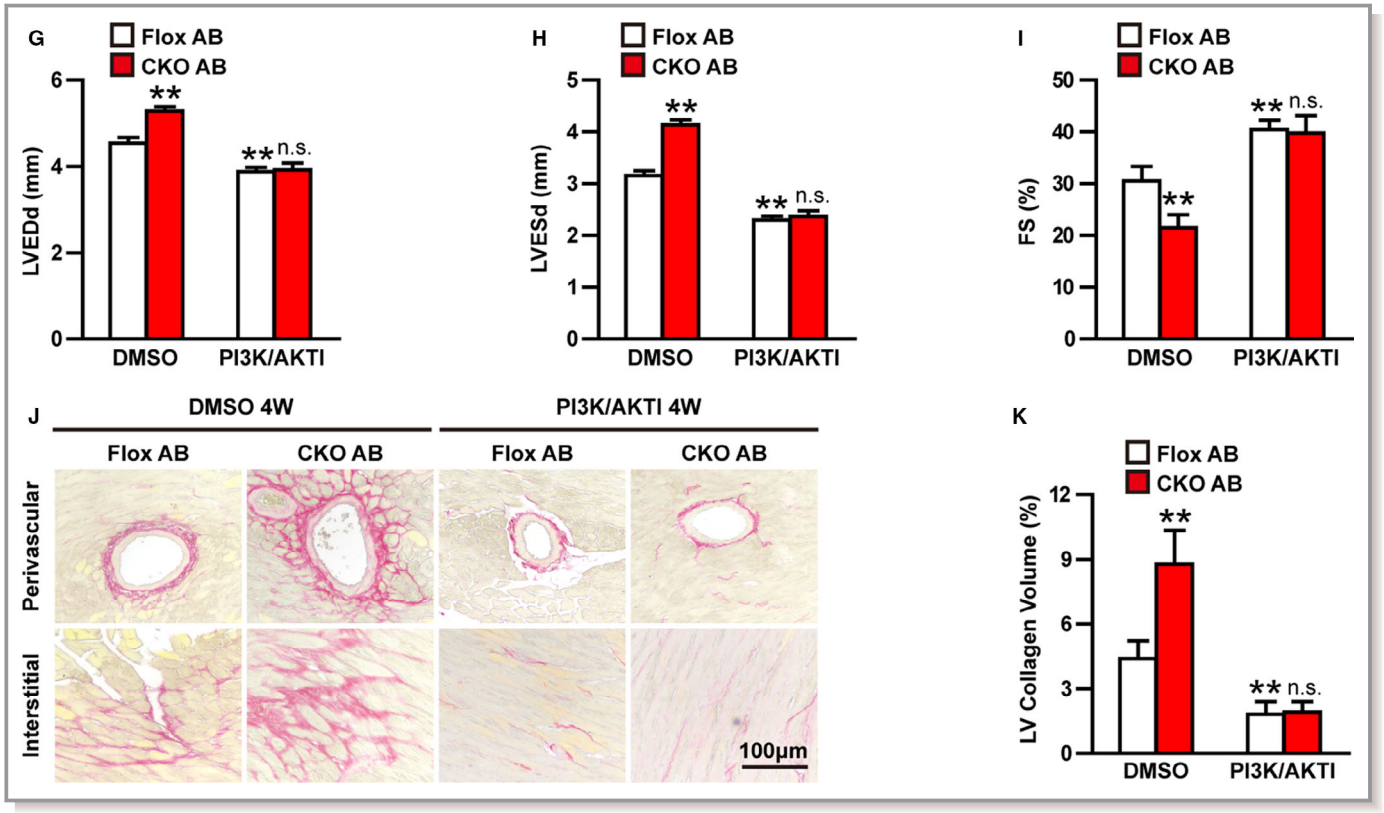

Figure 6. Continued

PHLDA3 CKO mice and PHLDA3 TG mice induced by pressure overload, which may be because of the effect of cardiomyocytes on fibroblasts partly through paracrine CTGF and other factors. Further analyses of the mechanisms revealed that the beneficial effect of PHLDA3 on cardiac hypertrophy was mainly dependent on blockade of the AKT signaling pathway. In addition, PHLDA3 protein expression was downregulated in hypertrophied mouse hearts and Ang II-treated cardiomyocytes. Collectively, these results indicated that PHLDA3 plays a vital role in the development of pathological cardiac hypertrophy and heart failure.

PHLDA3 was originally identified as a p53-inducible protein under stressed conditions[24,25] with 2 p53 binding motifs in its promoter and a PH domain that competes with AKT.[8] Previous study revealed that ablation of endogenous PHLDA3 results in enhanced AKT activity.[8] However, the phosphorylation level of AKT did not change under the sham- or PBS-treated basal state. Only in the AB or Ang II stimulation, down-regulation or up-regulation of PHLDA3, respectively promoted or inhibited AKT phosphorylation in vivo and in vitro. Therefore, in our study, the regulation of AKT by PHLDA3 in the pathological cardiac hypertrophy may be stress-dependent. Moreover, many studies have found that PHLDA3, as a tumor suppressor such as p53, is associated with a variety of tumors, particularly neuroendocrine tumors.[8,11–13,26] Decreased expression of PHLDA3 is correlated with tumorigenesis, disease progression and poor prognosis,[8,11–13,26] and the decrease in PHLDA3 expression may be because of the high frequency of loss of heterozygosity at the PHLDA3 gene locus and methylation of the PHLDA3 promoter.[11] Furthermore, PHLDA3 not only promoted P53-mediated renal tubular cell death but also increased its transcript and protein levels after cisplatin treatment.[14,15] In the present study, contrary to atrial natriuretic peptide expression, the expression of PHLDA3 was decreased in a time-dependent manner after AB or Ang II treatment, indicating that PHLDA3 serves as a potential biomarker of pathological cardiac hypertrophy in response to hypertrophic stimuli. In addition, PHLDA3 could regulate glucose metabolism,[11] impede somatic cell reprogramming,[27] impair the specification of hemangioblasts and vascular development,[28] and facilitate hepatocyte death induced by endoplasmic reticulum stress.[16] However, the effect of PHLDA3 in cardiovascular diseases remains unclear. In the present study, PHLDA3 mitigates pathological cardiac hypertrophy in vitro and in vivo. Hence, our findings uncovered the functional role of PHLDA3 as a negative regulator in pathological cardiac hypertrophy.

PHLDA3 functions as a PH domain-only protein and competes with another PH-domain-containing protein, AKT, for binding to membrane lipids, thereby impeding AKT

translocation to the cellular membrane and its activation.[8] Most of the biological functions of PHLDA3 have been shown to involve inhibiting AKT signaling through its PH domain. In the present study, as expected, the protective role of PHLDA3 in pathological cardiac hypertrophy induced by chronic pressure overload was still exerted by suppressing the AKT-mTOR-GSK3β-P70S6K signaling pathway. It is well known that the AKT signaling pathway plays an important role in cardiac hypertrophy, including both physiological cardiac hypertrophy and pathological cardiac hypertrophy.[23,29,30] Multiple studies have demonstrated that short-term activation of AKT initially promotes physiological hypertrophy,[31] whereas long-term activation causes pathological hypertrophy and cardiac dysfunction.[32,33] Moreover, previous studies have shown that sustained activation of AKT contributes to the transition from compensated cardiac hypertrophy to decompensated cardiac remodeling and heart failure, which involve multiple pathological changes, including alterations in coronary angiogenesis, cell size, and survival.[30,34] Thus, AKT is a pivotal target molecule that determines the benign and malignant progression of cardiac hypertrophy and the severity of pathological cardiac hypertrophy. As the downstream molecules of AKT, mTOR, and GSK3β, are phosphorylated by the activation of AKT.[35] Although a heart-specific deficiency of mTOR exacerbates pathological cardiac hypertrophy and accelerates the development of heart failure induced by pressure overload,[36] inhibition of mTOR with rapamycin treatment blunts the hypertrophic response in humans and in animal models.[37–39] Meanwhile, GSK3β is constitutively active under unstimulated conditions, while the activity of GSK3β is restricted by its level of phosphorylation.[40] Previous studies have shown that GSK3β is an endogenous negative regulator of cardiac hypertrophy,[41] and further studies have suggested that inhibition of Ser9 phosphorylation in GSK3β attenuates pressure overload-induced cardiac hypertrophy and heart failure.[42] Additionally, P70S6K, a downstream effector of mTOR, is also decreased in the regulation of cardiac hypertrophy with rapamycin,[37,38,43] which indicates that P70S6K is a crucial mediator of hypertrophy downstream of the AKT-mTOR cascade. Therefore, the pivotal role of the AKT-mTOR-GSK3β-P70S6K signaling pathway in the regulation of pathological cardiac hypertrophy and heart failure is self-evident. Aside from the present study, previous studies from our group and others have confirmed that many molecules act on cardiac remodeling by regulating the AKT signaling pathway.[18,44–47]

In conclusion, this study first demonstrates that PHLDA3 ameliorates pathological cardiac hypertrophy in vitro and in vivo mainly by inhibiting the AKT signaling pathway. These findings broaden our understanding of the functional roles of PHLDA3 and suggest that PHLDA3 may be a potential therapeutic target for pathological cardiac hypertrophy and heart failure.

Sources of Funding

This work was supported by grants from the National Natural Science Foundation of China (No. 81270184, No. 81670044, No. 81800252) and the Fundamental Research Funds for the Central Universities (No. 2042018kf0054, No. 2042019kf0096).

Disclosures

None.

References

1. Ziaeian B, Fonarow GC. Epidemiology and aetiology of heart failure. *Nat Rev Cardiol*. 2016;13:368–378.
2. Deng KQ, Zhao GN, Wang Z, Fang J, Jiang Z, Gong J, Yan FJ, Zhu XY, Zhang P, She ZG, Li H. Targeting transmembrane BAX inhibitor Motif containing 1 alleviates pathological cardiac hypertrophy. *Circulation*. 2018;137:1486–1504.
3. Deng KQ, Wang A, Ji YX, Zhang XJ, Fang J, Zhang Y, Zhang P, Jiang X, Gao L, Zhu XY, Zhao Y, Gao L, Yang Q, Zhu XH, Wei X, Pu J, Li H. Suppressor of IKKvarepsilon is an essential negative regulator of pathological cardiac hypertrophy. *Nat Commun*. 2016;7:11432.
4. Heineke J, Molkentin JD. Regulation of cardiac hypertrophy by intracellular signalling pathways. *Nat Rev Mol Cell Biol*. 2006;7:589–600.
5. Tham YK, Bernardo BC, Ooi JY, Weeks KL, McMullen JR. Pathophysiology of cardiac hypertrophy and heart failure: signaling pathways and novel therapeutic targets. *Arch Toxicol*. 2015;89:1401–1438.
6. van Berlo JH, Maillet M, Molkentin JD. Signaling effectors underlying pathologic growth and remodeling of the heart. *J Clin Invest*. 2013;123:37–45.
7. Frank D, Mendelsohn CL, Ciccone E, Svensson K, Ohlsson R, Tycko B. A novel pleckstrin homology-related gene family defined by Ipl/Tssc3, TDAG51, and Tih1: tissue-specific expression, chromosomal location, and parental imprinting. *Mamm Genome*. 1999;10:1150–1159.
8. Kawase T, Ohki R, Shibata T, Tsutsumi S, Kamimura N, Inazawa J, Ohta T, Ichikawa H, Aburatani H, Tashiro F, Taya Y. PH domain-only protein PHLDA3 is a p53-regulated repressor of Akt. *Cell*. 2009;136:535–550.
9. Yue F, Cheng Y, Breschi A, Vierstra J, Wu W, Ryba T, Sandstrom R, Ma Z, Davis C, Pope BD, Shen Y, Pervouchine DD, Djebali S, Thurman RE, Kaul R, Rynes E, Kirilusha A, Marinov GK, Williams BA, Trout D, Amrhein H, Fisher-Aylor K, Antoshechkin I, DeSalvo G, See LH, Fastuca M, Drenkow J, Zaleski C, Dobin A, Prieto P, Lagarde J, Bussotti G, Tanzer A, Denas O, Li K, Bender MA, Zhang M, Byron R, Groudine MT, McCleary D, Pham L, Ye Z, Kuan S, Edsall L, Wu YC, Rasmussen MD, Bansal MS, Kellis M, Keller CA, Morrissey CS, Mishra T, Jain D, Dogan N, Harris RS, Cayting P, Kawli T, Boyle AP, Euskirchen G, Kundaje A, Lin S, Lin Y, Jansen C, Malladi VS, Cline MS, Erickson DT, Kirkup VM, Learned K, Sloan CA, Rosenbloom KR, Lacerda de Sousa B, Beal K, Pignatelli M, Flicek P, Lian J, Kahveci T, Lee D, Kent WJ, Ramalho Santos M, Herrero J, Notredame C, Johnson A, Vong S, Lee K, Bates D, Neri F, Diegel M, Canfield T, Sabo PJ, Wilken MS, Reh TA, Giste E, Shafer A, Kutyavin T, Haugen E, Dunn D, Reynolds AP, Neph S, Humbert R, Hansen RS, De Bruijn M, Selleri L, Rudensky A, Josefowicz S, Samstein R, Eichler EE, Orkin SH, Levasseur D, Papayannopoulou T, Chang KH, Skoultchi A, Gosh S, Disteche C, Treuting P, Wang Y, Weiss MJ, Blobel GA, Cao X, Zhong S, Wang T, Good PJ, Lowdon RF, Adams LB, Zhou XQ, Pazin MJ, Feingold EA, Wold B, Taylor J, Mortazavi A, Weissman SM, Stamatoyannopoulos JA, Snyder MP, Guigo R, Gingeras TR, Gilbert DM, Hardison RC, Beer MA, Ren B; Mouse EC. A comparative encyclopedia of DNA elements in the mouse genome. *Nature*. 2014;515:355–364.
10. Fagerberg L, Hallstrom BM, Oksvold P, Kampf C, Djureinovic D, Odeberg J, Habuka M, Tahmasebpoor S, Danielsson A, Edlund K, Asplund A, Sjostedt E, Lundberg E, Szigyarto CA, Skogs M, Takanen JO, Berling H, Tegel H, Mulder J, Nilsson P, Schwenk JM, Lindskog C, Danielsson F, Mardinoglu A, Sivertsson A, von Feilitzen K, Forsberg M, Zwahlen M, Olsson I, Navani S, Huss M, Nielsen J, Ponten F, Uhlen M. Analysis of the human tissue-specific expression by genome-wide integration of transcriptomics and antibody-based proteomics. *Mol Cell Proteomics*. 2014;13:397–406.
11. Ohki R, Saito K, Chen Y, Kawase T, Hiraoka N, Saigawa R, Minegishi M, Aita Y, Yanai G, Shimizu H, Yachida S, Sakata N, Doi R, Kosuge T, Shimada K, Tycko B, Tsukada T, Kanai Y, Sumi S, Namiki H, Taya Y, Shibata T, Nakagama H. PHLDA3 is a novel tumor suppressor of pancreatic neuroendocrine tumors. *Proc Natl Acad Sci USA*. 2014;111:E2404–E2413.

12. Christgen M, Noskowicz M, Heil C, Schipper E, Christgen H, Geffers R, Kreipe H, Lehmann U. IPH-926 lobular breast cancer cells harbor a p53 mutant with temperature-sensitive functional activity and allow for profiling of p53-responsive genes. *Lab Invest*. 2012;92:1635–1647.
13. Yoo NJ, Kim YR, Lee SH. Expressional and mutational analysis of PHLDA3 gene in common human cancers. *Pathology*. 2011;43:510–511.
14. Lee CG, Kang YJ, Kim HS, Moon A, Kim SG. Phlda3, a urine-detectable protein, causes p53 accumulation in renal tubular cells injured by cisplatin. *Cell Biol Toxicol*. 2015;31:121–130.
15. Lee CG, Kim JG, Kim HJ, Kwon HK, Cho IJ, Choi DW, Lee WH, Kim WD, Hwang SJ, Choi S, Kim SG. Discovery of an integrative network of microrna and transcriptomics changes for acute kidney injury. *Kidney Int*. 2014;86:943–953.
16. Han CY, Lim SW, Koo JH, Kim W, Kim SG. PHLDA3 overexpression in hepatocytes by endoplasmic reticulum stress via IRE1-Xbp1s pathway expedites liver injury. *Gut*. 2016;65:1377–1388.
17. Mottillo S, Filion KB, Genest J, Joseph L, Pilote L, Poirier P, Rinfret S, Schiffrin EL, Eisenberg MJ. The metabolic syndrome and cardiovascular risk a systematic review and meta-analysis. *J Am Coll Cardiol*. 2010;56:1113–1132.
18. Liu X, Yang Q, Zhu LH, Liu J, Deng KQ, Zhu XY, Liu Y, Gong J, Zhang P, Li S, Xia H, She ZG. Carboxyl-terminal modulator protein ameliorates pathological cardiac hypertrophy by suppressing the protein kinase B signaling pathway. *J Am Heart Assoc*. 2018;7:e008654. DOI: 10.1161/JAHA.118.008654.
19. Ji YX, Zhang P, Zhang XJ, Zhao YC, Deng KQ, Jiang X, Wang PX, Huang Z, Li H. The ubiquitin E3 ligase TRAF6 exacerbates pathological cardiac hypertrophy via TAK1-dependent signalling. *Nat Commun*. 2016;7:11267.
20. Chen L, Huang J, Ji Y, Zhang X, Wang P, Deng K, Jiang X, Ma G, Li H. Tripartite motif 32 prevents pathological cardiac hypertrophy. *Clin Sci (Lond)*. 2016;130:813–828.
21. Oka T, Maillet M, Watt AJ, Schwartz RJ, Aronow BJ, Duncan SA, Molkentin JD. Cardiac-specific deletion of Gata4 reveals its requirement for hypertrophy, compensation, and myocyte viability. *Circ Res*. 2006;98:837–845.
22. Hill JA, Olson EN. Cardiac plasticity. *N Engl J Med*. 2008;358:1370–1380.
23. Shimizu I, Minamino T. Physiological and pathological cardiac hypertrophy. *J Mol Cell Cardiol*. 2016;97:245–262.
24. Day KR, Jagadeeswaran P. Microarray analysis of prothrombin knockdown in zebrafish. *Blood Cells Mol Dis*. 2009;43:202–210.
25. Kerley-Hamilton JS, Pike AM, Li N, DiRenzo J, Spinella MJ. A p53-dominant transcriptional response to cisplatin in testicular germ cell tumor-derived human embryonal carcinoma. *Oncogene*. 2005;24:6090–6100.
26. Muroi H, Nakajima M, Satomura H, Takahashi M, Yamaguchi S, Sasaki K, Yokobori T, Miyazaki T, Kuwano H, Kato H. Low PHLDA3 expression in oesophageal squamous cell carcinomas is associated with poor prognosis. *Anticancer Res*. 2015;35:949–954.
27. Qiao M, Wu M, Shi R, Hu W. PHLDA3 impedes somatic cell reprogramming by activating Akt-GSK3beta pathway. *Sci Rep*. 2017;7:2832.
28. Wang X, Li J, Yang Z, Wang L, Li L, Deng W, Zhou J, Wang L, Xu C, Chen Q, Wang QK. Phlda3 overexpression impairs specification of hemangioblasts and vascular development. *FEBS J*. 2018;285:4071–4081.
29. Kemi OJ, Ceci M, Wisloff U, Grimaldi S, Gallo P, Smith GL, Condorelli G, Ellingsen O. Activation or inactivation of cardiac Akt/mTOR signaling diverges physiological from pathological hypertrophy. *J Cell Physiol*. 2008;214:316–321.
30. Dorn GW II, Force T. Protein kinase cascades in the regulation of cardiac hypertrophy. *J Clin Invest*. 2005;115:527–537.
31. Shiojima I, Yefremashvili M, Luo Z, Kureishi Y, Takahashi A, Tao J, Rosenzweig A, Kahn CR, Abel ED, Walsh K. Akt signaling mediates postnatal heart growth in response to insulin and nutritional status. *J Biol Chem*. 2002;277:37670–37677.
32. Matsui T, Nagoshi T, Rosenzweig A. Akt and PI 3-kinase signaling in cardiomyocyte hypertrophy and survival. *Cell Cycle*. 2003;2:220–223.
33. Chaanine AH, Hajjar RJ. AKT signalling in the failing heart. *Eur J Heart Fail*. 2011;13:825–829.
34. Aoyagi T, Matsui T. Phosphoinositide-3 kinase signaling in cardiac hypertrophy and heart failure. *Curr Pharm Des*. 2011;17:1818–1824.
35. Matsui T, Rosenzweig A. Convergent signal transduction pathways controlling cardiomyocyte survival and function: the role of PI 3-kinase and Akt. *J Mol Cell Cardiol*. 2005;38:63–71.
36. Zhang D, Contu R, Latronico MV, Zhang J, Rizzi R, Catalucci D, Miyamoto S, Huang K, Ceci M, Gu Y, Dalton ND, Peterson KL, Guan KL, Brown JH, Chen J, Sonenberg N, Condorelli G. MTORC1 regulates cardiac function and myocyte survival through 4E-BP1 inhibition in mice. *J Clin Invest*. 2010;120:2805–2816.
37. Shioi T, McMullen JR, Tarnavski O, Converso K, Sherwood MC, Manning WJ, Izumo S. Rapamycin attenuates load-induced cardiac hypertrophy in mice. *Circulation*. 2003;107:1664–1670.
38. McMullen JR, Sherwood MC, Tarnavski O, Zhang L, Dorfman AL, Shioi T, Izumo S. Inhibition of mTOR signaling with rapamycin regresses established cardiac hypertrophy induced by pressure overload. *Circulation*. 2004;109:3050–3055.
39. Soesanto W, Lin HY, Hu E, Lefler S, Litwin SE, Sena S, Abel ED, Symons JD, Jalili T. Mammalian target of rapamycin is a critical regulator of cardiac hypertrophy in spontaneously hypertensive rats. *Hypertension*. 2009;54:1321–1327.
40. Doble BW, Woodgett JR. GSK-3: tricks of the trade for a multi-tasking kinase. *J Cell Sci*. 2003;116:1175–1186.
41. Hardt SE, Sadoshima J. Negative regulators of cardiac hypertrophy. *Cardiovasc Res*. 2004;63:500–509.
42. Matsuda T, Zhai P, Maejima Y, Hong C, Gao S, Tian B, Goto K, Takagi H, Tamamori-Adachi M, Kitajima S, Sadoshima J. Distinct roles of GSK-3alpha and GSK-3beta phosphorylation in the heart under pressure overload. *Proc Natl Acad Sci USA*. 2008;105:20900–20905.
43. Shiojima I, Sato K, Izumiya Y, Schiekofer S, Ito M, Liao R, Colucci WS, Walsh K. Disruption of coordinated cardiac hypertrophy and angiogenesis contributes to the transition to heart failure. *J Clin Invest*. 2005;115:2108–2118.
44. Deng KQ, Li J, She ZG, Gong J, Cheng WL, Gong FH, Zhu XY, Zhang Y, Wang Z, Li H. Restoration of circulating MFGE8 (milk fat globule-EGF factor 8) attenuates cardiac hypertrophy through inhibition of Akt pathway. *Hypertension*. 2017;70:770–779.
45. Zhao QD, Viswanadhapalli S, Williams P, Shi Q, Tan C, Yi X, Bhandari B, Abboud HE. NADPH oxidase 4 induces cardiac fibrosis and hypertrophy through activating Akt/mTOR and NFkappaB signaling pathways. *Circulation*. 2015;131:643–655.
46. Sundaresan NR, Vasudevan P, Zhong L, Kim G, Samant S, Parekh V, Pillai VB, Ravindra PV, Gupta M, Jeevanandam V, Cunningham JM, Deng CX, Lombard DB, Mostoslavsky R, Gupta MP. The sirtuin SIRT6 blocks IGF-Akt signaling and development of cardiac hypertrophy by targeting c-Jun. *Nat Med*. 2012;18:1643–1650.
47. Chen K, Gao L, Liu Y, Zhang Y, Jiang DS, Wei X, Zhu XH, Zhang R, Chen Y, Yang Q, Kioka N, Zhang XD, Li H. Vinexin-beta protects against cardiac hypertrophy by blocking the Akt-dependent signalling pathway. *Basic Res Cardiol*. 2013;108:338.

Supplemental Material

Figure S1. Representative echo images and assessments of the mice hearts.

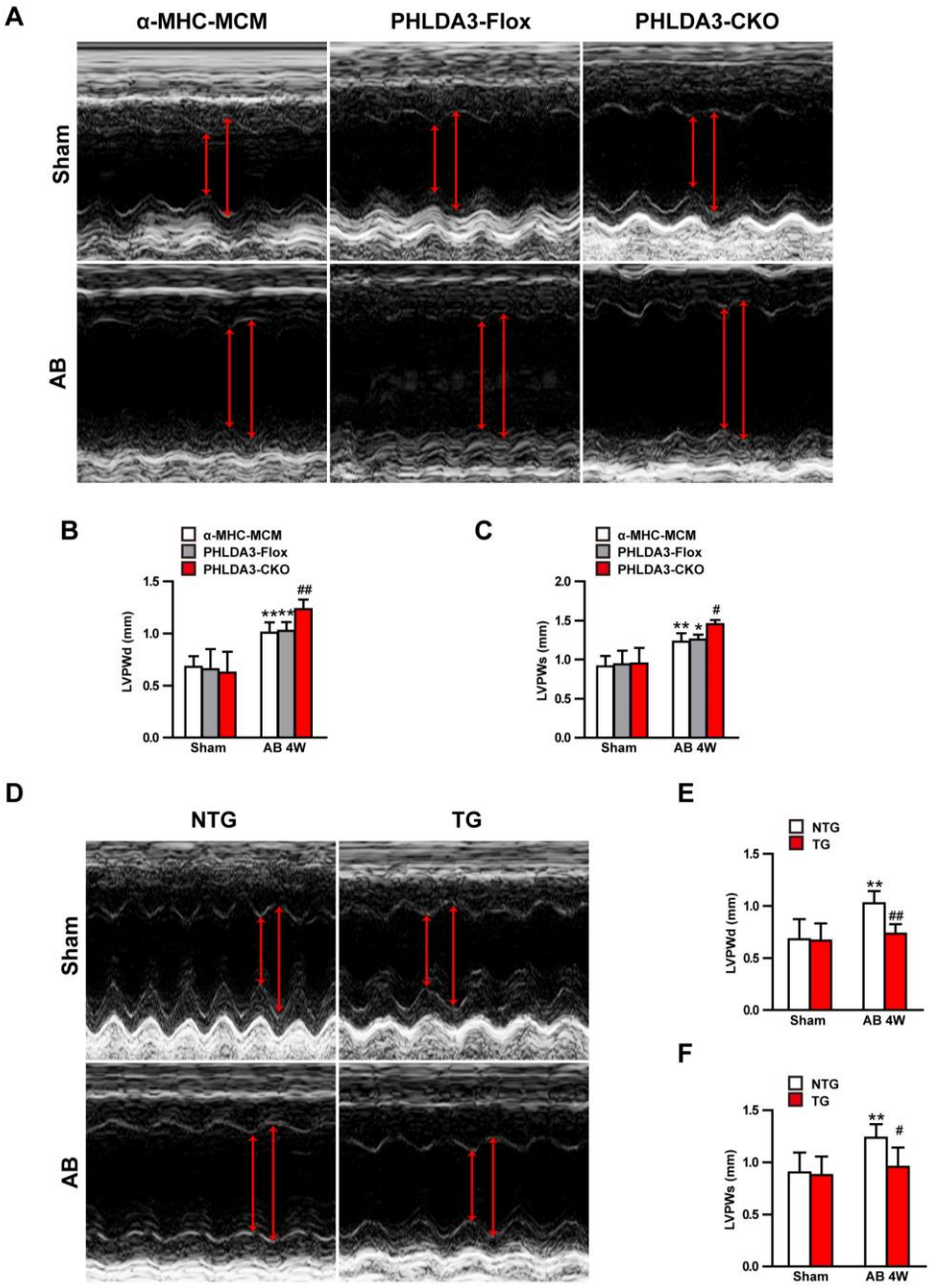

A, Representative echo images of the α-MHC-MCM, PHLDA3-Flox and PHLDA3-CKO mice before and after AB. **B** and **C**, Echocardiographic assessment of the LVPWd (**B**) and LVPWs (**C**) in the indicated groups at 4 weeks after sham or AB surgery (n=8 mice per group). **D**, Representative echo images of the NTG and TG mice before and after AB. **E** and **F**, Echocardiographic assessment of the LVPWd (**E**) and LVPWs (**F**) in the indicated groups at 4 weeks after sham or AB surgery (n=8

mice per group). *P<0.05 or **P<0.01 vs α-MHC-MCM sham or PHLDA3-Flox sham or NTG sham; $^{\#}P$<0.05 or $^{\#\#}P$<0.01 vs α-MHC-MCM AB or PHLDA3-Flox AB or NTG AB in **B, C**, **E**, and **F**. By Tamhane's T2 analysis (**B**) or Bonferroni post hoc analysis (**C**, **E** and **F**). AB indicates aortic banding; PHLDA3-CKO, cardiomyocyte-specific conditional PHLDA3 knockout mice; PHLDA3-Flox, PHLDA3$^{loxP/loxP}$ (PHLDA3-Flox) mice; NTG, nontransgenic mice; TG, conditional PHLDA3 transgenic mice; LVPWd, left ventricular posterior wall thickness at end diastole; LVPWs, left ventricular posterior wall thickness at end systole; PHLDA3, pleckstrin homology-like domain family A, member 3.

Figure S2. PHLDA3 deficiency fails to regulate physiological cardiac hypertrophy.

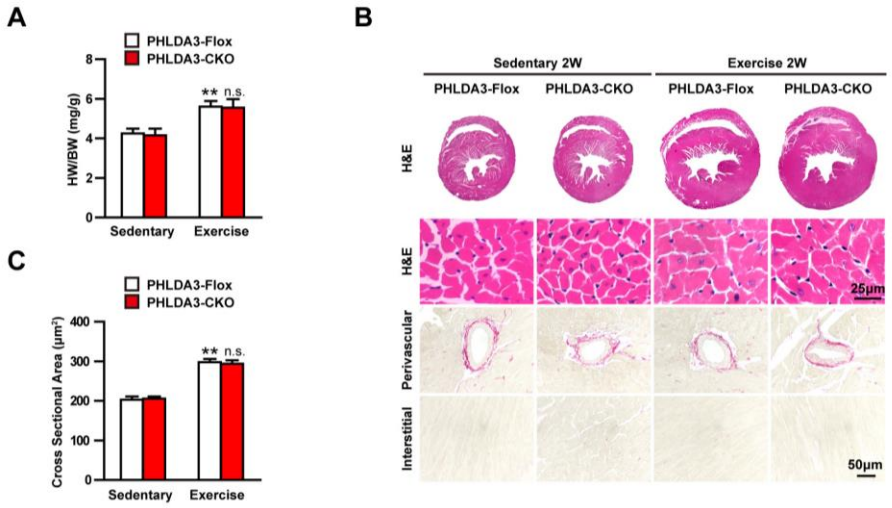

A, The ratios of HW/BW in the indicated groups (n=8 mice per experimental group). **B**, Representative H&E staining images of the gross morphology (the first row) and left ventricular muscle of hearts (the second row; scale bar, 25 μm) or PSR (the third and fourth row; scale bars, 50 μm) from the indicated groups (n=5 mice per experimental group). **C**, Statistical results for the cell cross-sectional areas in the indicated groups (n≥100 cells per experimental group). $^{**}P<0.01$ vs. PHLDA3-Flox sedentary; n.s. indicates no significant difference. By Bonferroni post hoc analysis (**A** and **C**). PHLDA3-CKO indicates cardiomyocyte-specific conditional PHLDA3 knockout mice; PHLDA3-Flox, PHLDA3$^{loxP/loxP}$ (PHLDA3-Flox) mice; HW, heart weight; BW, body weight; H&E, hematoxylin and eosin; W, weeks; PHLDA3, pleckstrin homology-like domain family A, member 3.

Figure S3. Echocardiographic assessment of the EF in the indicated groups at 4 weeks after sham or AB surgery (n=11 to 13 mice per group).

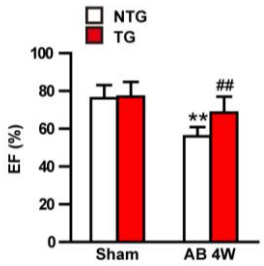

**P<0.01 vs NTG sham; ##P<0.01 vs NTG AB. By Bonferroni post hoc analysis. AB indicates aortic banding; NTG, nontransgenic mice; TG, conditional PHLDA3 transgenic mice; EF, ejection fraction; W, weeks.

Figure S4. Cardiomyocyte-specific PHLDA3 overexpression blunts the hypertrophic response induced by AB after 8 weeks.

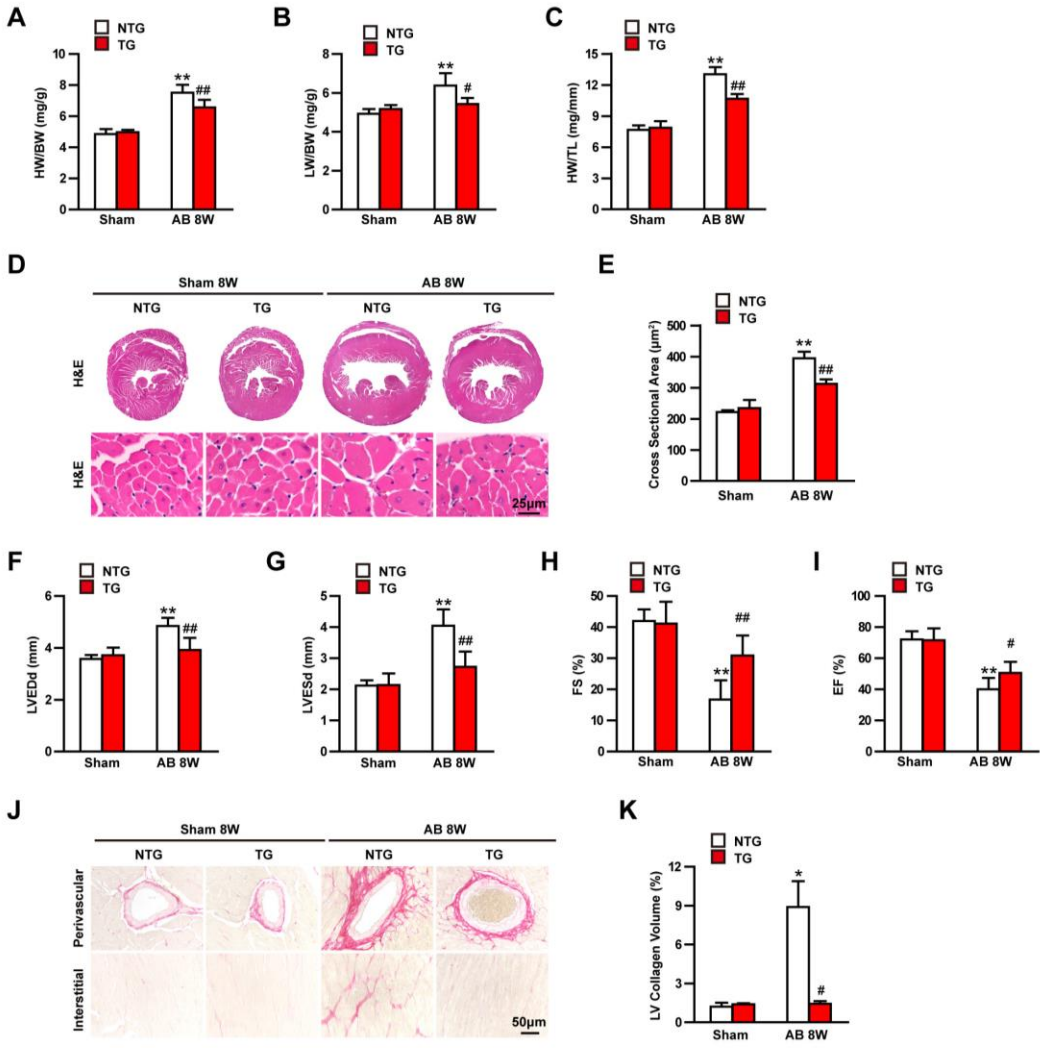

A-**C**, Statistical results of the ratios of HW/BW (A), LW/BW (B), and HW/TL (C) in NTG and TG mice at 8 weeks after sham or AB surgery (n=8 mice per group). **D**, Representative H&E staining images of the gross morphology and left ventricular muscle of hearts from the indicated groups (n=5 mice per group; scale bar, 25 μm). **E**, Statistical results of the cardiomyocyte cross-sectional area from the indicated groups (n≥100 cells per group). **F**-**I**, Echocardiographic assessment of the LVEDd (**F**), LVESd (**G**), FS (**H**), and EF (**I**) in the indicated groups at 8 weeks after sham or AB surgery (n=8 mice per group). **J**, Representative images of PSR staining of

perivascular and myocardial interstitial regions of the hearts from the indicated groups (n=5 mice per group; scale bar, 50 μm). **K**, Statistical results of fibrotic areas from the indicated groups (n>30 fields per group). **P*<0.05 or ***P*<0.01 vs NTG sham; $^{\#}P$<0.05 or $^{\#\#}P$<0.01 vs NTG AB in **A**-**C**, **E**, **F**-**I**, **K**. By Tamhane's T2 analysis (**B**, **F**, **G** and **K**) or Bonferroni post hoc analysis (**A**, **C**, **E**, **H** and **I**). AB indicates aortic banding; NTG, nontransgenic mice; TG, conditional PHLDA3 transgenic mice; HW, heart weight; LW, lung weight; BW, body weight; TL, tibia length; W, weeks; H&E, hematoxylin and eosin; LVEDd, left ventricle end-diastolic diameter; LVESd, left ventricle end-systolic diameter; FS, fractional shortening; EF, ejection fraction; LV, left ventricle; PHLDA3, pleckstrin homology-like domain family A, member 3.

Figure S5. Representative images of cardiomyocytes stained with the α-actinin antibody.

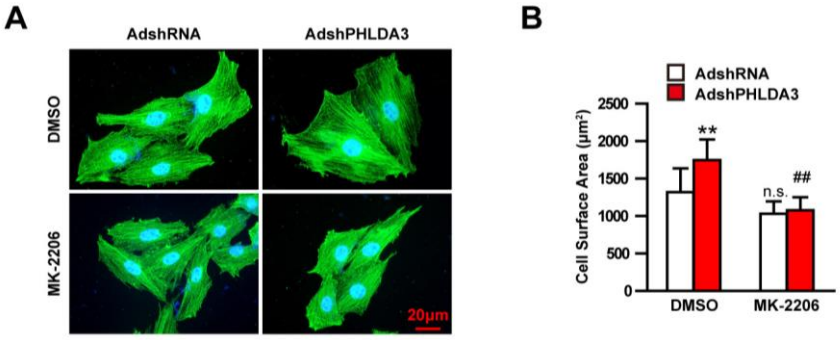

A, AdshPHLDA3-infected NRCMs were treated with MK-2206 (an AKT inhibitor, 1 μmol/L) for 48 hours. Scale bars, 20 μm. **B**, Cardiomyocyte size was quantified. n=3 independent experiments. $^{**}P<0.01$ vs AdshRNA+Ang II+DMSO, $^{\#\#}P<0.01$ vs AdshPHLDA3+Ang II+DMSO. n.s. indicates no significant difference. n>50 cells per group. By Tamhane's T2 analysis (**B**). AdshRNA indicates adenoviral short hairpin RNA; AdshPHLDA3, adenoviral vectors harboring the PHLDA3 short hairpin RNA; DMSO, dimethyl sulfoxide; MK-2206, an AKT inhibitor; PHLDA3, pleckstrin homology-like domain family A, member 3.